The yeast H^+-ATPase Pma1 promotes Rag/Gtr-dependent TORC1 activation in response to H^+-coupled nutrient uptake

Elie Saliba[1], Minoas Evangelinos[1#], Christos Gournas[1#], Florent Corrillon[1], Isabelle Georis[2], and Bruno André[1,*]

[1] Molecular Physiology of the Cell, Université Libre de Bruxelles (ULB), Biopark, 6041 Gosselies, Belgium
[2] Institut de Recherches Microbiologiques J.-M. Wiame, 1070 Brussels, Belgium
[#] These authors contributed equally to this work
* For correspondence : Bruno.Andre@ulb.ac.be

Abstract

The yeast Target of Rapamycin Complex 1 (TORC1) plays a central role in controlling growth. How amino acids and other nutrients stimulate its activity via the Rag/Gtr GTPases remains poorly understood. We here report that the signal triggering Rag/Gtr-dependent TORC1 activation upon amino-acid uptake is the coupled H^+ influx catalyzed by amino-acid/H^+ symporters. H^+-dependent uptake of other nutrients, ionophore-mediated H^+ diffusion, and inhibition of the vacuolar V-ATPase also activate TORC1. As the increase in cytosolic H^+ elicited by these processes stimulates the compensating H^+-export activity of the plasma membrane H^+-ATPase (Pma1), we have examined whether this major ATP-consuming enzyme might be involved in TORC1 control. We find that when the endogenous Pma1 is replaced with a plant H^+-ATPase, H^+ influx or increase fails to activate TORC1. Our results show that H^+ influx coupled to nutrient uptake stimulates TORC1 activity and that Pma1 is a key actor in this mechanism.

Introduction

The Target of Rapamycin Complex 1 (TORC1) plays a pivotal role in controlling cell growth in probably all eukaryotic organisms. It operates by integrating upstream signals such as growth factors (GFs) and nutrients to modulate, by phosphorylation, multiple downstream effectors, mostly proteins involved in anabolic processes (e. g. protein synthesis, ribosome biogenesis) or catabolic processes (e. g. autophagy, bulk endocytosis of plasma membrane transporters) (González and Hall, 2017; Powis and De Virgilio, 2016; Saxton and Sabatini, 2017). The central role of TORC1 in regulating cell growth is illustrated by the many reported cases of mTORC1 dysfunction associated with diseases including cancers (Eltschinger and Loewith, 2016; Saxton and Sabatini, 2017).

In human cells, GFs and amino acids are key signals of mTORC1 regulation. GFs act through activation of Rheb, a GTPase present at the lysosomal membrane that stimulates mTORC1 activity (Durán and Hall, 2012; Zheng et al., 2014). Amino acids such as leucine and arginine act via a complex of two GTPases, namely RagA or B and RagC or D, to promote recruitment of mTORC1 to the lysosome, where it is

activated by Rheb. The heterodimeric Rag GTPase complex recruits mTORC1 to the lysosome when RagA/B is bound to GTP and RagC/D to GDP (Kim et al., 2008; Sancak et al., 2008). The activity of GTPases is typically modulated by GTPase Activating Proteins (GAPs) and Guanine nucleotide Exchange Factors (GEFs). Recent studies have aimed to identify these GAPs and GEFs and their upstream regulators and to better understand how these factors are controlled in response to variations in the cytosolic concentrations of amino acids and/or to their transport across the plasma or lysosomal membrane (González and Hall, 2017; Powis and De Virgilio, 2016; Saxton and Sabatini, 2017). Importantly, Sestrin and Castor proteins have recently been found to act, respectively, as cytosolic leucine and arginine sensors. When bound to their specific amino acids, these sensor proteins lose the ability to inhibit GATOR2, a negative modulator of the GATOR1 GAP complex which inhibits RagA/B, and this results in TORC1 activation (Wolfson and Sabatini, 2017). Specific lysosomal amino acid transporters and the V-ATPase complex also contribute importantly to mTORC1 control (Goberdhan et al., 2016; Zoncu et al., 2011). All this illustrates the complexity of the mechanisms through which amino acids regulate mTORC1 activity.

The TOR kinase that is part of TORC1 was originally identified in yeast, after isolation of dominant *TOR* mutations conferring resistance to rapamycin (Rap) (Heitman et al., 1991; Loewith and Hall, 2011). The protein components of TORC1, the RagA/B and C/D proteins, and their upstream GATOR-type regulatory complexes also exist in yeast (Hatakeyama and De Virgilio, 2016; Loewith and Hall, 2011). For instance, RagA/B and RagC/D correspond, respectively, to the yeast Gtr1 and Gtr2 proteins, which are part of a vacuole-associated complex (EGO) (Dubouloz et al., 2005) similar to the Rag-binding Ragulator of human cells (Sancak et al., 2010). When cells are grown in nutrient-rich medium, yeast TORC1 is active and stimulates by phosphorylation a wide variety of proteins. It notably stimulates the Sch9 kinase (Urban et al., 2007) under conditions promoting anabolic functions and cell growth. Active TORC1 also inhibits the Tap42-PP2A phosphatase, which stimulates autophagy, stress resistance, and nitrogen (N) transport and utilization (Loewith and Hall, 2011). In contrast, TORC1 is inhibited in N-starved and Rap-treated cells, so that anabolic processes, including protein synthesis, are inhibited and cell responses such as autophagy, bulk endocytosis of transporters, utilization of secondary N sources,

and stress resistance are stimulated (Hatakeyama and De Virgilio, 2016; Loewith and Hall, 2011). One Tap42-PP2A target protein is the protein kinase Npr1 (Nitrogen permease reactivator 1), which is phospho-inhibited when TORC1 is active (Schmidt et al., 1998). Once Npr1 is inhibited, various permeases of nitrogenous compounds undergo intrinsic inactivation (Boeckstaens et al., 2014; 2015) or downregulation via ubiquitylation, endocytosis, and degradation (MacGurn et al., 2011; Merhi and André, 2012).

Stimulation of TORC1 activity in yeast is usually monitored by visualizing the degree of Sch9 and/or Npr1 kinase phosphorylation. Sch9 and Npr1 are moderately phosphorylated in cells grown on a poor N source such as proline, but hyperphosphorylated upon addition of a preferential N source such as glutamine (Gln) or NH_4^+ (Schmidt et al., 1998; Stracka et al., 2014; Urban et al., 2007). In a study using Sch9 phosphorylation as readout, addition of any amino acid to proline-grown cells was found to result in rapid but transient Rag/Gtr-dependent TORC1 activation, whereas longer-term TORC1 activation was observed only upon addition of an N source supporting optimal growth, e. g. Gln or NH_4^+, and it appeared not to depend on the Rag GTPases (Stracka et al., 2014). Furthermore, sustained activation of TORC1 in response to NH_4^+ is impaired in mutant cells lacking the glutamate dehydrogenases involved in assimilation of NH_4^+ into amino acids (Fayyad-Kazan et al., 2016; Merhi and André, 2012). The upstream signals and molecular mechanisms involved in activation of yeast TORC1 in response to amino acid uptake and/or assimilation remain poorly known. For instance, although Gln behaves as a key signal for sustained TORC1 stimulation (Crespo et al., 2002; Stracka et al., 2014), no Gln sensor has been identified to date, and yeast seems to lack Sestrin and Castor proteins. Furthermore, no study has evidenced any particular role of vacuolar amino acid transporters in TORC1 regulation. The yeast leucyl-tRNA synthetase is reported to play a role in sensing balanced levels of isoleucine, leucine, and valine and to act as a GEF for Gtr1 (Bonfils et al., 2012), whereas the equivalent mammalian enzyme is proposed to control mTORC1 as a GAP for RagD (Han et al., 2012). On the basis of current knowledge, it would thus seem that the upstream signals and mechanisms controlling TORC1 according to the N or amino acid supply conditions might differ significantly between yeast and human cells.

The present study began with an unexpected observation regarding the uptake of β-alanine into yeast cells: this amino acid, which cannot be used as an N source (i.e. it is not a source of amino acids), stimulates TORC1 activity. Analysis of this effect has revealed that the general signal triggering Rag/Gtr-dependent activation of TORC1 in response to amino acid uptake is the influx of H^+ coupled to transport via H^+/amino-acid symporters. We further show that the Pma1 H^+-ATPase establishing the H^+ gradient at the plasma membrane is essential to this TORC1 activation, and suggest that Pma1 modulates TORC1 via signaling.

Results

Uptake of β-alanine via the Gap1 permease causes Rag/Gtr-dependent TORC1 activation without increasing internal pools of amino acids

In cells growing under poor N supply conditions (e. g. in a medium containing proline as sole N source), the yeast general amino acid permease Gap1 is active and stable at the plasma membrane. Under these conditions, TORC1 is only moderately active (Schmidt et al., 1998). Activation of TORC1 upon NH_4^+ uptake and assimilation into amino acids triggers Gap1 ubiquitylation, followed by its endocytosis and degradation in the vacuole (Merhi and André, 2012). Thanks to isolation of a Gap1 mutant insensitive to this TORC1-dependent ubiquitylation, we have shown that substrate transport by Gap1 can also trigger Ub-dependent endocytosis and degradation of this transporter (Ghaddar et al., 2014b). This type of control, shared with other transporters of fungal and non-fungal species, probably enables cells to avoid excess uptake of external compounds (Gournas et al., 2016). To further investigate, without interference from the TORC1-dependent pathway, the mechanism of transport-elicited Gap1 ubiquitylation we sought to identify a Gap1 amino acid substrate unable to activate TORC1. We focused on beta-alanine (β-ala) and confirmed its reported status as a Gap1 substrate (Stolz and Sauer, 1999) by comparing the uptake of [^{14}C]-β-ala (0.5 mM) in proline-grown wild-type and *gap1Δ* mutant cells (Fig. 1A). β-Ala, however, cannot sustain growth when used as sole N source, i.e. it cannot serve as a source of amino acids (Fig. 1A). This contrasts with 4-aminobutyrate (GABA), an amino acid differing from β-ala by a single additional CH_2

group (Fig. 1A) and whose catabolism depends on a specific GABA transaminase (Andersen et al., 2007). We thus tested whether β-ala transport by Gap1 triggers ubiquitylation and downregulation of the transporter. This proved to be the case, as addition of β-ala (0.5 mM) caused the appearance, above the immunodetected Gap1 signal, of two slowly migrating bands that were not observed with the non-ubiquitylable Gap1(K9R,K16R) mutant (Fig. 1B). Upon β-ala addition, furthermore, Gap1 initially present at the cell surface underwent endocytosis and targeting to the vacuole, whereas Gap1(K9R,K16R) remained stable at the plasma membrane (Fig. 1C). An inactive Gap1 mutant (Gap1-126) (Ghaddar et al., 2014b) failed to be ubiquitylated and downregulated upon β-ala addition (Figs. 1B, 1C). These results are those expected if β-ala elicits Gap1 ubiquitylation specifically via the transport-elicited pathway. Yet we sought to make sure that β-ala does not activate TORC1. To our surprise, addition of β-ala to proline-grown cells caused a typical manifestation of TORC1 activation: a Rap-sensitive reduction of the electrophoretic mobility of HA-tagged Npr1, indicative of increased phosphorylation via TORC1 (Merhi and André, 2012; Schmidt et al., 1998) (Fig. 1D). β-Ala similarly caused a Rap-sensitive increase in the phosphorylation of Sch9 kinase residue Thr737 (Fig. 1E), a known TORC1 target (Urban et al., 2007). It thus seemed that activation of TORC1, largely impaired in the *gap1Δ* mutant (Figs. 1D, 1E), could contribute to the observed β-ala-induced downregulation of Gap1. This assumption was confirmed in additional experiments (Fig. 1-figure supplement 1). Gap1-mediated uptake of β-ala thus results in TORC1 activation. We therefore hypothesized that, although β-ala cannot be used as an N source, it might be converted to certain amino acids capable of stimulating TORC1. β-Ala uptake, however, was found not to increase the intracellular concentrations of individual amino acids, measured in cell extracts, apart from that of β-ala itself (Fig. 1F). We next tested whether this β-ala-induced activation of TORC1 involves the Rag A/B and C/D GTPases, encoded by the *GTR1* and *GTR2* genes, respectively. Increased phosphorylation of Npr1 upon β-ala addition was indeed impaired in *gtr1Δ gtr2Δ* mutant cells (Fig. 1G), and this effect was not due to reduced uptake of β-ala (Fig. 1H). We conclude that Gap1-mediated uptake of β-ala elicits TORC1 activation via

the Rag GTPases, and that this effect is not due to conversion of intracellular β-ala to other amino acids.

Uptake of β-ala via the endogenous Put4 or the heterologous HcGap1 permease also promotes TORC1 activation

Gap1 has been reported to be a "transceptor", i.e. a protein combining the properties of transporters and receptors, capable of activating protein kinase A (PKA) in a cAMP-independent manner (Donaton et al., 2003). According to this model, conformational changes of Gap1, triggered by binding and/or transport of amino acids, would stimulate a PKA-targeting signaling pathway (Schothorst et al., 2013). We thus hypothesized that this transceptor function of Gap1 might also promote TORC1 activation in a Rag/Gtr-dependent manner. This hypothesis is potentially supported by a previous report that Gap1 interacts with Gtr2 (Gao and Kaiser, 2006). An alternative view is that β-ala entering cells through Gap1 might be detected by a cytosolic amino acid sensor capable of promoting TORC1 activation. To explore these possibilities, we tested whether β-ala uptake via another permease might also activate TORC1. Confirming a previous prediction (Gournas et al., 2015), we found the high-affinity proline permease Put4 also to catalyze β-ala transport. This contribution of Put4 was visible at least in proline-free media, such as a medium where the sole N source was urea (another poor N source). Under these conditions, the *gap1Δ* mutant displayed residual uptake of β-ala (2 mM), and this uptake was abolished in the *gap1Δ put4Δ* mutant (Fig. 2A). Importantly, this Put4-dependent β-ala uptake was associated with a Rap-sensitive hyperphosphorylation of Npr1 (Fig. 2B). We next expressed in the *gap1Δ* mutant a heterologous amino acid transporter known to be active in *S. cerevisiae*, namely the Gap1 permease of the fungus *Hebeloma cylindrosporum* (Wipf et al., 2002). HcGap1 shares ~30% sequence identity with Gap1 and Put4. In proline-grown *gap1Δ* cells, HcGap1 restored high β-ala uptake activity, roughly similar to that conferred by Put4 to urea-grown cells (Fig. 2C). Remarkably, this uptake of β-ala was also associated with Rap-sensitive hyperphosphorylation of Npr1 (Fig. 2D). In conclusion, transport of β-ala via endogenous Gap1 and/or Put4 or via the heterologous HcGap1 permease elicits TORC1 activation. Although these observations do not rule out the possibility that all

three tested permeases might function as transceptors, they seem to favor the view that intracellular β-ala itself, or the process of its transport across the plasma membrane, stimulates TORC1 activity.

Uptake of arginine via an endogenous or a heterologous permease stimulates TORC1 even if arginine catabolism is impaired

Uptake of arginine (Arg) by proline-grown cells is known to be mediated by Gap1 and the arginine-specific permease Can1 (Wiame et al., 1985). Consistently, we measured high Arg uptake activity in the wild type and in *gap1Δ* and *can1Δ* single mutants, but none in the *gap1Δ can1Δ* double mutant (Fig. 3A). According to a previous report, Can1, in contrast to Gap1, does not stimulate PKA upon substrate transport (Donaton et al., 2003). This suggests that Can1 does not function as a transceptor. We thus sought to determine whether Arg transport via Gap1 or Can1 alone supports TORC1 activation. Arg uptake into wild-type cells was indeed found to induce Rap-sensitive Npr1 hyperphosphorylation (Figs. 3A, 3B). This response was impaired in the *gtr1Δ gtr2Δ* mutant, an effect not due to decreased Arg uptake (Fig. 3B). Arg-elicited TORC1 activation also resulted in Sch9 phosphorylation (Fig. 3C), as previously reported (Stracka et al., 2014). Increased phosphorylation of Npr1 upon Arg addition was also detected in *gap1Δ* and *can1Δ* single mutants, but not in the *gap1Δ can1Δ* strain (Fig. 3A). This shows that both permeases can promote Arg-induced TORC1 activation. We next expressed HcGap1 in the *gap1Δ can1Δ* strain and found it to restore high Arg uptake (Fig. 3D) associated with Rap-sensitive Npr1 hyperphosphorylation (Fig. 3E). Arginine catabolism requires arginase (Car1) (Wiame et al., 1985), so a *car1* mutant fails to grow on Arg as sole N source (Fig. 3F). Arg addition to the *car1* mutant also resulted in Rap-sensitive Npr1 hyperphosphorylation (Fig. 3G). In conclusion, TORC1 is activated upon Arg uptake via the endogenous Gap1 and/or Can1 or the heterologous HcGap1 permease. This activation of TORC1 involves the Rag GTPases and occurs even if Arg is not catabolized.

H^+ influx coupled to transport promotes Rag/Gtr-dependent stimulation of TORC1

The simplest way to explain the above observations is that intracellular β-ala and Arg

are detected by one or several internal amino acid sensors promoting Rag/Gtr-dependent TORC1 activation. These sensors could, for instance, act like the human Castor and Sestrin proteins, recently shown to function as arginine and leucine sensors, respectively, and to modulate upstream regulators of mTORC1 (Wolfson and Sabatini, 2017). These sensor proteins, however, do not seem to exist in yeast. Furthermore, one would not expect a cytosolic sensor capable of activating TORC1 in response to β-ala. Alternatively, a TORC1-activating signal might arise from a common feature of the permease-mediated Arg and β-ala transport reactions. In yeast, transport by secondary active plasma membrane transporters is coupled to H^+ influx. This transport is thus driven by the plasma membrane H^+ gradient established by the Pma1 H^+-ATPase. We therefore hypothesized that an influx of H^+ coupled to amino acid uptake might initiate a signal stimulating TORC1 activity. To evaluate this hypothesis, we first checked that the β-ala and Arg transporters tested above are H^+-symporters. In support of this view, incubation of cells with the FCCP protonophore caused a strong reduction of β-ala uptake via Gap1, Put4, or HcGap1 and of Arg uptake via Gap1, Can1, or HcGap1 (Figs. 4A, 4B). Furthermore, each permease was rapidly inhibited when the cells were shifted to glucose-free medium (Figs. 4A, 4B), a condition known to cause rapid inhibition of the Pma1 H^+-ATPase and thus collapse of the plasma membrane H^+ gradient (Kane, 2016). Hence, as expected, all four permeases analyzed in our study, including HcGap1, behave as H^+-symporters. We next examined whether active uptake of another metabolite, not present in the growth medium, also elicits Rag/Gtr-dependent TORC1 activation. We chose cytosine, whose uptake via the Fcy2 permease is known to be coupled to H^+ influx (Pinson et al., 1997). Interestingly, addition of cytosine did cause rapid activation of TORC1, as judged by increased Npr1 and Sch9 phosphorylation (Figs. 4C, 4D). Furthermore, this cytosine-elicited TORC1 activation was largely impaired in the *gtr1Δ gtr2Δ* mutant (Fig. 4E). Cytosine can be used as sole N source, and thus as a source of amino acids. Yet in an *fcy1* mutant lacking cytosine deaminase and thus unable to use cytosine as an N source, Npr1 was still phosphorylated upon cytosine addition, unless Rap was also present (Fig. 4F). H^+-coupled uptake of cytosine thus stimulates TORC1 in a Rag/Gtr-dependent manner, even when the nucleobase is not

assimilated into amino acids. This observation is compatible with the proposed view that H^+ influx is the signal initiating TORC1 stimulation.

To further assess this model, we sought to analyze the activity of TORC1 upon equivalent uptake of the same external compound by either a facilitator or an H^+-coupled symporter. Hexoses including fructose are known to enter cells via several Hxt transporters that function as facilitators (Wieczorke et al., 1999). Yet particular *S. cerevisiae* strains were reported to also express an H^+-coupled specific fructose transporter termed Fsy1 (Galeote et al., 2010; Rodrigues de Sousa et al., 2004). We thus used the *hxt* null strain, lacking the *HXT1 to -17* and *GAL2* genes and therefore unable to assimilate hexoses (Wieczorke et al., 1999), in which we expressed the *FSY1* gene behind its own promoter, or none hexose transporter gene, and we analyzed in parallel the wild-type (from which the *hxt* null mutant derives) expressing the endogenous Hxt facilitators. The strains were initially grown on maltose as *hxt* null cells can utilize this disaccharide. They were then shifted for a few hours to ethanol because the *FSY1* gene is more highly expressed on this carbon source (Rodrigues de Sousa et al., 2004). As in previous experiments, the N source was proline. Using these growth conditions, we measured equivalent ^{14}C-fructose uptake in Hxt- and Fsy1-expressing cells (Fig. 4G). None significant fructose uptake was detected in the *hxt* null mutant, as expected (Fig. 4G). Furthermore, fructose uptake via Fsy1 was inhibited in the presence of FCCP, which was not the case when it was mediated by the Hxt facilitators (Fig. 4H). We finally applied these growth and fructose uptake conditions to assay TORC1 activity. We observed a Rap-sensitive increased phosphorylation of Sch9, upon fructose uptake, in Fsy1-expressing cells. Such a TORC1 activation was not observed in the wild-type incorporating fructose via the Hxt facilitators neither the *hxt* null mutant expressing none fructose transporter (Fig. 4 I). TORC1 activation in response to fructose uptake thus only occurred when this transport was coupled to H^+ influx. This result fully supports the view that it is the H^+ influx that generates the signal of TORC1 activation.

H^+ diffusion via a protonophore promotes Rag/Gtr-dependent stimulation of TORC1

In all above experiments, TORC1 thus seems activated in response to the H^+-influx coupled to a nutrient transport reaction. We next determined whether the sole diffusion of H^+ via a protonophore like FCCP also elicits TORC1 activation. Using a strain stably expressing pHluorin, we first observed that the ionophore caused the cytosolic pH to drop to about 6.1, the pH of the buffered growth medium (Fig. 5A). Remarkably, this rapid acidification of the cytosol coincided with hyperphosphorylation of Npr1, and this response was inhibited by Rap (Fig. 5B). Hence, H^+ influx mediated by a protonophore also results in TORC1 stimulation. Yet this TORC1 activation, intriguingly, did not lead to increased phosphorylation of Sch9 (Fig. 5C). A likely explanation is that an additional control elicited when the cytosol becomes too acidic (a stressful condition) impedes phosphorylation of Sch9 by activated TORC1. This is in keeping with a previous report that when the cytosolic pH drops to values around 6 (as occurs under glucose starvation or when expression of the Pma1 H^+-ATPase is repressed), the action of TORC1 on Sch9 is inhibited, whereas nitrogen control of the Gat1 and Gln3 transcription factors via TORC1 remains unaltered (Dechant et al., 2014).

The activation of TORC1 upon H^+ influx mediated by FCCP, thus visible in immunoblots for HA-Npr1, was largely impaired in the *gtr1Δ gtr2Δ* strain (Fig. 5D), indicating that it is Rag/Gtr-dependent. The multisubunit SEACIT complex antagonizes TORC1 by acting as a GAP on the Gtr1 GTPase, and its function is itself negatively controlled by the multisubunit SEACAT complex (Panchaud et al., 2013a; 2013b). To determine whether these GATOR-like upstream regulators of Gtr1 are involved in H^+ influx-elicited TORC1 activation, FCCP was added to cells lacking Seh1 or Iml1, components of the SEACAT and SEACIT complexes, respectively (Panchaud et al., 2013a; 2013b). TORC1 activation was largely impaired in the *seh1Δ* mutant (Fig. 5E). In the *iml1Δ* mutant, a high basal phosphorylation of HA-Npr1 was detected, as expected, and FCCP did not significantly further increase this phosphorylation, at least during the first minutes after its addition (Fig. 5F). These results indicate that the SEACIT/SEACAT upstream regulators of Gtr1 are involved in H^+-influx-elicited stimulation of TORC1 activity. We also noticed that the amount of HA-Npr1 is much reduced in *seh1Δ* mutant cells, and a similar effect though less pronounced was observed in the *gtr1Δ gtr2Δ* strain (Figs. 1G, 4E, 5D). This suggests

that HA-Npr1 abundance is influenced by the activation state of TORC1. What is also evident from the analysis of the above mutants is that phosphorylation of HA-Npr1 increased after prolonged incubation with FCCP (Figs. 5D, 5E, 5F). It thus seems that FCCP stimulates another mechanism of TORC1 activation that is not dependent on the Rag/Gtr GTPases. For instance, longer incubation of FCCP could promote release of amino acids from the vacuole or mitochondria, and this could promote TORC1 activation independently of Gtr1/2. It has in fact been reported that the vacuole-associated Pib2 protein containing a FYVE domain acts in parallel with Gtr1 to promote TORC1 activation (Kim and Cunningham, 2015; Varlakhanova et al., 2017). Furthermore, in an *in vitro* TORC1 kinase assay using isolated vacuoles, the addition of glutamine was found to stimulate TORC1 activity in a manner dependent on Pib2 but not Gtr1 (Tanigawa and Maeda, 2017). We thus also analyzed the role of Pib2 and found that HA-Npr1 is normally hyperphosphorylated after FCCP addition to *pib2Δ* mutant cells (Fig. 5G).

In conclusion, the above experiments indicate that H^+ influx mediated even by a protonophore elicits a cellular response resulting in Rag/Gtr-dependent, Pib2-independent, TORC1 activation. They further suggest that if the cytosol becomes too acidic, an additional control likely impedes Sch9 phosphorylation by activated TORC1.

Inhibition of the vacuolar V-ATPase activates TORC1

We observed that addition of amino acids, cytosine, or NH_4^+ to growing cells does not detectably change their cytosolic pH (data not shown). This was expected, given the high buffering capacity of the cytosol and the compensating H^+ efflux activity of the Pma1 H^+-ATPase, which is stimulated under acidic conditions as long as glucose is present (Eraso and Gancedo, 1987; Ullah et al., 2012). We then examined whether an increase of cytosolic H^+, imposed without changing the composition of the external medium, might also lead to TORC1 activation. An H^+ increase can in principle be caused by inhibition of the vacuolar V-ATPase, as this enzymatic complex catalyzes ATP-dependent uptake of H^+ into the vacuole in order to acidify the organelle, to compensate for the constant H^+ efflux mediated by H^+-coupled vacuolar transporters, and to control the cytosolic pH (Kane, 2016). We thus tested

the effects of two inhibitors of the V-ATPase, concanamycin A (CMA) and bafilomycin A (BAF) (Fig. 6). Addition of CMA to proline-grown cells did not significantly change the cytosolic pH of the cells (Fig. 6A). This suggests that Pma1-dependent efflux and the buffering capacity of the cytosol prevented the expected increase in cytosolic H^+. BAF addition did cause a slight but significant drop in the cytosolic pH, suggesting that this treatment caused stronger inhibition of the V-ATPase (Fig. 6E). Remarkably, both CMA and BAF treatment resulted in stimulation of TORC1 activity, as judged by Rap-sensitive hyperphosphorylation of Npr1 (Fig. 6B and Fig. 6F, respectively) and by a transient increase in Sch9 phosphorylation (Fig. 6C and Fig. 6G, respectively). No increase in Npr1 phosphorylation was detected in either CMA- or BAF-treated *gtr1Δ gtr2Δ* mutant cells (Figs. 6D and 6H, respectively). We conclude that inhibition of the V-ATPase is associated with efficient Rag/Gtr-dependent stimulation of TORC1 activity, even when this inhibition is not sufficient to cause a detectable lowering of the cytosolic pH.

TORC1 activation in response to increased cytosolic H^+ requires the Pma1 H^+-ATPase

Activation of TORC1 in the above-described situations (H^+ influx, increased in cytosolic H^+) might involve an uncharacterized sensor of intracellular H^+, capable of transmitting this signal to TORC1. Alternatively, the Pma1 H^+-ATPase might control TORC1 activity upon sensing H^+ influx or increase in cytosol. For instance, Pma1 activity increases under acidic conditions, and this coincides with a reduction of its Km for ATP, possibly via allosteric control (Eraso and Gancedo, 1987; Ullah et al., 2012). We hypothesized that the particular state adopted by the H^+-ATPase in response to increased H^+ might stimulate certain factors controlling TORC1 activity. To test this possibility, we thought of expressing in yeast, instead of the endogenous Pma1, a heterologous H^+-ATPase known to be catalytically active in yeast. We reasoned that if TORC1 activation depends on a signaling capability of Pma1, an H^+-ATPase from a distant species should fail to activate TORC1 in response to an increase in cytosolic H^+.

According to previous reports, several plant H^+-ATPases are active when expressed in yeast strains where the essential *PMA1* gene and its non-essential

paralog *PMA2* (expressed to a much lower level) are deleted or repressed (Morsomme et al., 2000; Palmgren and Christensen, 1994). The wild-type forms of these plant H^+-ATPases typically compensate only partially for the lack of Pma1. It is possible, however, to isolate mutant derivatives sustaining faster growth, particularly on low-pH media where cells need high H^+-ATPase activity to maintain a neutral cytosolic pH (Morsomme et al., 2000). For instance, the H^+-ATPase Pma4 of tobacco (*Nicotiana plumbaginifolia*) restores limited growth to a *pma1Δ pma2Δ* double-null mutant. A truncated Pma4 protein called $Pma4^{882ochre}$, lacking the last 71 C-terminal amino acids as a result of an ochre nonsense mutation in codon 882 of the *PMA4* gene, is able to support faster growth of yeast *pma1Δ pma2Δ* cells (Luo et al., 1999). We thus studied TORC1 activation in cells expressing either the endogenous *PMA1* gene or the tobacco plant $PMA4^{822ochre}$ gene. As most the above experiments were carried out with strains having the ∑1278b background, we first isolated a *GAL1-PMA1 pma2Δ* derivative of this strain, where the *PMA1* gene is placed under the control of the galactose-inducible, glucose-repressible *GAL1* promoter. This strain can grow on galactose but not glucose, unless it contains a plasmid expressing the endogenous *PMA1* gene or the tobacco $PMA4^{822ochre}$ gene under the control of the *PMA1* promoter (Fig. 7A). We cultured *GAL-PMA1 pma2Δ* cells expressing *PMA1* or $PMA4^{822ochre}$ on glucose proline medium, as in the above-described experiments. We found cells expressing $PMA4^{822ochre}$ to grow more slowly (Fig. 7B). This shows that the mutant plant H^+-ATPase does not fully compensate for the lack of Pma1. Accordingly, compared to the cytosolic pH of *PMA1*-expressing cells, that of $PMA4^{822ochre}$-expressing cells was slightly lower (Fig. 7C). H^+-coupled uptake of β-ala (1 mM) was also significantly lower in the latter cells (data not shown). We therefore lowered the concentration of β-ala provided to *PMA1*-expressing cells in order to reach an uptake rate equivalent to that measured in $PMA4^{822ochre}$-expressing cells (Figs. 7D, 7F). As expected, and whichever gene was expressed, [^{14}C]-β-ala uptake was inhibited after a brief treatment of the cells with FCCP. This shows that in both cases, β-ala uptake is coupled to H^+ influx (Figs. 7D, 7F). Upon transfer of the cells to a glucose-free medium, uptake of β-ala into *PMA1*-expressing cells was also strongly reduced (Figs. 7D, 7F). This was expected, since

Pma1 is inhibited under these conditions. This reduction was much less pronounced in *PMA4*^{822ochre}-expressing cells (Figs. 7D, 7F). This result can be readily explained by the fact that inactivation of H^+-ATPases upon glucose starvation, a regulation conserved between yeast and plant H^+-ATPases, requires a C-terminal auto-inhibitory region which the truncated protein Pma4^{822ochre} lacks (Morsomme et al., 2000; Portillo, 2000). Next, under conditions of equal H^+-coupled β-ala uptake into *PMA1*- and *PMA4*^{822ochre}-expressing cells, we analyzed TORC1 activity. Phosphorylation of Npr1 was found to increase moderately upon addition of β-ala at low concentration (0.1 mM) to *PMA1*-expressing cells, but this variation was significant, as judged by its sensitivity to Rap (Fig. 7E). Remarkably, no increase in Npr1 phosphorylation was detected in *PMA4*^{822ochre}-expressing cells (Fig. 7E). Furthermore, basal phosphorylation of Npr1 in these cells did not increase, despite the lower pH of their cytosol (Figs. 7E, 7C). Non-activation of TORC1 in *PMA4*^{822ochre}-expressing cells was even clearer when Sch9 phosphorylation was used as readout (Fig. 7G). Basal phosphorylation of Sch9 before β-ala addition was also reduced in *PMA4*^{822ochre}-expressing cells (Fig. 7G). Non-activation of TORC1 in *PMA4*^{822ochre}-expressing cells upon β-ala uptake was also observed in the background of another strain deleted of both *PMA1* and *PMA2* (Fig. 7-figure supplement 1). We next analyzed TORC1 activation after addition of glutamine, leucine, or arginine, each activation being deficient in the *gtr1Δ gtr2Δ* strain (Fig. 7-figure supplement 2). As with β-ala, the external concentration of each amino acid was first adjusted to reach equivalent uptake in *PMA1*- and *PMA4*^{822ochre}-expressing cells. Using these conditions, we observed a Rap-sensitive activation of TORC1 in the cells expressing *PMA1* but not in those expressing *PMA4*^{822ochre} (Fig. 7-figure supplement 2). We also analyzed TORC1 activation upon FCCP addition. In both *PMA1*- and *PMA4*^{822ochre}-expressing cells, as expected, the ionophore caused a rapid drop in the cytosolic pH, to a value close to the pH of the buffered external medium (Fig. 7C). Also as expected, this induced strong hyperphosphorylation of Npr1 in control *PMA1*-expressing cells (Fig. 7H). In contrast, FCCP addition did not increase Npr1 phosphorylation in *PMA4*^{822ochre}-expressing cells (Fig. 7H). Similar results were obtained after treatment with BAF: Npr1 phosphorylation was found to increase in

PMA1-expressing but not in *PMA4*^{822ochre}-expressing cells (Fig. 7I). These results show that the endogenous Pma1 H^+-ATPase plays an essential role in Rag/Gtr-dependent TORC1 activation in response to increased cytosolic H^+. The importance of Pma1 in stimulating TORC1 activity was also illustrated by the ability of *PMA1*-expressing cells to resume growth following exposure to Rap, whereas *PMA4*^{822ochre}-expressing cells failed to do so (Fig. 7J).

It has been reported that the Rag GTPases are not required for sustained activation of TORC1 in the presence of NH_4^+ (Stracka et al., 2014). In support of this view, NH_4^+ addition to proline-grown cells caused Rap-sensitive hyperphosphorylation of Npr1 in both wild-type and *gtr1Δ gtr2Δ* mutant cells (Fig. 7K). Furthermore, sustained TORC1 activation after NH_4^+ addition is reported to depend on the enzymes converting NH_4^+ to glutamate (Fayyad-Kazan et al., 2016; Merhi and André, 2012), the main N donor in amino acid biogenesis reactions. Interestingly, upon NH_4^+ addition to proline-grown cells, we found TORC1 to be properly activated by NH_4^+ regardless of the H^+-ATPase produced (Pma1 or the plant Pma4^{822ochre}) (Fig. 7K). This result shows that TORC1 can be properly activated in *PMA4*^{822ochre}-expressing cells. It also suggests that Pma1 is required for TORC1 activation in response to H^+ influx but not to an increase in internal amino acids.

Discussion

Uptake of amino acids into N-deprived yeast cells causes Rag/Gtr-dependent activation of TORC1. The actual signal and the underlying mechanism of this cellular response remain unknown. Our study shows that it is the H^+ influx coupled to transport by H^+/amino-acid symporters that triggers this activation. A similar response is observed upon H^+-dependent uptake of cytosine, or even fructose, but not when an equivalent amount of fructose enters the cells via passive transport systems. The activation of TORC1 can even be elicited by diffusion of extracellular H^+ via a protonophore or by inactivation of the vacuolar V-ATPase (which also causes an increase in cytosolic H^+). We further show that TORC1 activation in response to an H^+ influx and/or an increase in cytosolic H^+ requires the Rag GTPases encoded by the *GTR* genes. It, however, does not require the Pib2 protein recently shown to act in

parallel with the Rag/Gtr proteins to activate TORC1. Finally, we show that the Pma1 H^+-ATPase plays a central role in this TORC1 activation pathway.

Yeast cells typically adapt to starvation for any nutrient by reducing TORC1 activity. This is probably because mechanisms capable of sensing the nutritional status of the cell impede the activation of TORC1, and not just because H^+-coupled uptake of this nutrient potentially dropped. This reduction of TORC1 activity typically coincides with increased synthesis of large amounts of high-affinity H^+-symporters able to assimilate replenishing compounds, e. g. Gap1 for amino acids, Pho84 for phosphate, Sul1 and Sul2 for sulfate, Zrt1 for zinc, Fcy2 for cytosine, and Fur4 for uracil. Furthermore, many permeases for the non-limiting nutrients likely undergo parallel increased endocytosis and degradation as such response was observed in rapamycin-treated cells (Crapeau et al., 2014). The consequence of this permease reconfiguration at the plasma membrane is a probable overall reduction of H^+ influx. Our results suggest that the H^+-symporters that are derepressed under starvation conditions are potentially able to reactivate TORC1 once their substrate becomes available again in the medium. In other words, H^+ influx via these transporters could provide a general signal for reactivating TORC1 upon relief from diverse starvation conditions. On the other hand, sustained activation of TORC1 probably requires efficient assimilation of the internalized nutrient. Accordingly, longer-term TORC1 activation after addition of a preferential N source such as NH_4^+ is reported to require glutamine accumulation and/or synthesis (Stracka et al., 2014). The influx of H^+ coupled to uptake of any growth-limiting nutrient might thus provide a general signal for rapid, transient TORC1 reactivation in order to prepare cells for subsequent growth acceleration or restart once the nutrient has been properly assimilated. It could also contribute to the reactivation of TORC1 observed upon addition of glucose to glucose-starved cells, as although glucose enters cells via Hxt facilitators it also reactivates Pma1 in turn driving the H^+-coupled uptake of amino acids and other nutrients.

Uptake of amino acids by N-starved cells is also reported to elicit transient activation of PKA, resulting in stimulation of trehalase by phosphorylation (Donaton et al., 2003). According to current models, PKA could be activated via a signaling pathway stimulated by Gap1 acting as a transceptor, and a similar function has been

described for other H^+-coupled nutrient transporters found to be derepressed under particular starvation conditions (Schothorst et al., 2013). Yet the mechanisms underlying this signaling remain unknown. It is tempting to envisage an alternative model according to which the signal eliciting PKA activation is the H^+ influx coupled to the nutrient uptake reaction, as in the case of TORC1. This model is worth considering, since addition of FCCP to N-starved cells results in stimulation of trehalase activity (Fig. 5-figure supplement 1).

A previous study reported that addition of excess Gln to proline-grown cells causes a rapid, transient activation of TORC1, that is defective in the *gtr1Δ* mutant, followed by a more sustained TORC1 activity, still observed in *gtr1Δ* cells (Stracka et al., 2014). This Gtr1-independent TORC1 activation is reminiscent of the situation described in mouse cells, where Gln activates mTORC1 in a manner independent of RagA and RagB (Jewell et al., 2015). Similarly, direct addition of Gln to isolated vacuoles elicits TORC1 activation *in vitro* in a Gtr1-independent manner (Tanigawa and Maeda, 2017). In contrast, this response requires the Pib2 protein proposed to act in parallel with Gtr1 to activate TORC1 (Kim and Cunningham, 2015; Varlakhanova et al., 2017). These observations suggest that Gln uptake first elicits a transient, Gtr1-dependent activation of TORC1, and we propose that the signal of this early activation is the H^+ influx coupled to Gln transport. The subsequent sustained activation of TORC1, in contrast, is suggested to be promoted by the intracellular accumulation of Gln (Stracka et al., 2014). The actual function of Pib2 in this process needs further investigation. The same applies to Gtr1/2 because, while sustained TORC1 activation normally occurs after Gln addition to *gtr1Δ* cells (Stracka et al., 2014), we failed to observe it in the double *gtr1Δ gtr2Δ* mutant, in keeping with another study (Varlakhanova et al., 2017).

We have found the Sch9 kinase to be stimulated by TORC1 in response to an increase in cytosolic H^+. This observation is interesting, in the light of the recent finding that Sch9 contributes to pH homeostasis by controlling the assembly and activity of the vacuolar V-ATPase (Wilms et al., 2017). This is relevant because the latter, together with the plasma membrane H^+-ATPase, contributes importantly to controlling the cytosolic pH (Kane, 2016). Yet according to other reports, Sch9 phosphorylation and cell growth are reduced when the cytosol becomes acidic (e. g.

559 after a drop to a pH near 6), for instance under glucose starvation or when Pma1
560 synthesis is reduced (Dechant et al., 2014; Orij et al., 2012; Ullah et al., 2012). It thus
561 seems that even though Sch9 is activated by an H^+ influx and/or by an increase in
562 cytosolic H^+, it is inhibited when the cytosol becomes too acidic, and this causes
563 growth inhibition. In FCCP-treated cells, accordingly, TORC1 appears to be efficiently
564 activated (as judged by hyperphosphorylation of the Npr1 kinase), but this is not
565 accompanied by Sch9 phosphorylation. This suggests that a particular mechanism
566 sensitive to acidic conditions hampers Sch9 phosphorylation by activated TORC1.
567 Such a control seems physiologically relevant, as acidification of the cytosol is
568 stressful for the cell and stimulation of growth under these conditions would be
569 inappropriate. Accordingly, other stresses are reported to promote
570 dephosphorylation of Sch9 without affecting the TORC1-regulated Tap42-PP2A
571 branch controlling Npr1 phosphorylation (Hughes Hallett et al., 2014).

572 A key question raised by our work is: what is the molecular mechanism
573 responsible for stimulation of TORC1 activity in response to H^+ influx and/or an
574 increase in cytosolic H^+? Our data indicate that the plasma membrane Pma1 H^+-
575 ATPase plays a central role in this cellular response. Specifically, TORC1 activity fails
576 to be stimulated in response to H^+-coupled uptake of amino acids, ionophore-
577 mediated H^+ diffusion, or inhibition of the V-ATPase in cells producing the tobacco
578 plant $Pma4^{822ochre}$ instead of Pma1. Furthermore, these cells display a strongly
579 reduced ability to restart growth after exposure to rapamycin. At least two models
580 can be proposed to account for these observations. On the one hand, non-activation
581 of TORC1 might result indirectly from the inability of $Pma4^{822ochre}$ to fully compensate
582 for the lack of Pma1 activity. We did find $PMA4^{822ochre}$-expressing cells to grow more
583 slowly and their cytosol to be slightly acidic. This might trigger adaptive feedback
584 mechanisms impeding TORC1 reactivation. Yet in $PMA4^{822ochre}$-expressing cells we
585 found TORC1 to be properly activated after NH_4^+ addition, and this shows that
586 TORC1 activity can be efficiently stimulated at least via the Rag/Gtr-independent
587 pathway seemingly responding to internal amino acids (Stracka et al., 2014).
588 Alternatively, the essential role of Pma1 in TORC1 activation in response to H^+ influx
589 might reflect the ability of Pma1 to stimulate a signaling pathway controlling TORC1
590 activity. For instance, the activity of Pma1 is known to increase when the

591 concentration of H^+ in the cytosol rises, and this control involves a decreased Km for
592 ATP (Eraso and Gancedo, 1987; Ullah et al., 2012). This activity increase also likely
593 occurs when protons are co-transported with nutrients via plasma membrane H^+-
594 symporters. This stimulation of Pma1 activity, possibly involving a conformational
595 change of the H^+-ATPase, might be transmitted to cytosolic factors that would in
596 turn modulate TORC1 activity. A role of Pma1 in signaling to TORC1 is attractive,
597 because Pma1 is the main ATP-consuming enzyme of yeast and is thus ideally
598 positioned for sensing cellular ATP levels. Furthermore, as mentioned above, Pma1
599 stimulation by H^+ influx could also give cells a general mechanism for sensing relief
600 from starvation for any nutrient and for reactivating TORC1 in response to this relief.
601 Other observations support a role of Pma1 in signaling to TORC1. For instance,
602 TORC1 inhibition has been observed when Pma1 synthesis is reduced (Dechant et al.,
603 2014). Furthermore, yeast TORC1 is rapidly inhibited under glucose starvation
604 (Urban et al., 2007), this coinciding with polymerization of the kinase complex into a
605 single, vacuole-associated cylindrical structure (Prouteau et al., 2017). Although a
606 specific mechanism involving phosphorylation of the Kog1 subunit is reported to
607 contribute to this TORC1 inhibition (Hughes Hallett et al., 2015), a role of Pma1
608 might also be considered, as this H^+-ATPase is subject to rapid and reversible auto-
609 inhibition under these conditions (Portillo et al., 1989; Serrano, 1983). Interestingly,
610 a recent study reported that TORC1 is required for full activity of Pma1 (Mahmoud et
611 al., 2017), suggesting the existence of some crosstalk between Pma1 and TORC1. The
612 model that Pma1 is capable of controlling TORC1 via signaling also seems reasonable
613 in the light of previous works showing that the Na^+/K^+-ATPase of animals cells, a P-
614 type ATPase structurally similar to Pma1 and other H^+-ATPases, is engaged in
615 dynamic interactions with other proteins, including the Src tyrosine kinase. The
616 interaction with Src is modulated by the conformation of the ion pump and initiates
617 signal transduction processes (Cui and Xie, 2017). As the cytosolic region of the
618 Na^+/K^+-ATPase directly interacting with Src (Lai et al., 2013) is relatively well
619 conserved in the yeast H^+-ATPase, we introduced several substitutions in this Pma1
620 region to potentially disrupt possible interactions with other factors. These Pma1
621 variants, however, behaved normally in TORC1 activation assays.

In conclusion, our results show that cytosolic H^+ and Pma1 are major actors in TORC1 activation in response to active nutrient uptake. They also raise the interesting possibility that Pma1 might control TORC1 via signaling. Further work is needed to evaluate this model, which would open important prospects for work on nutritional signaling in yeast and other organisms.

Materials and Methods

Key Resources Table				
Reagent type (species) or resource	**Designation**	**Source or reference**	**Identifiers**	**Additional information**
antibody	anti-GFP (mouse monoclonal)	Roche	11814460001 ; RRID : AB_390913	(1:10000)
antibody	anti-Pma1 (rabbit polyclonal)	(De Craene et al., 2001)	RRID : AB_2722567	(1:5000)
antibody	anti-HA (12CA5) (mouse monoclonal)	Roche	11583816001 ; RRID : AB_514506	(1:5000)
antibody	anti-Pgk (mouse monoclonal)	Invitrogen	459250 ; RRID : AB_221541	(1:10000)
antibody	anti-(P)T737-Sch9 (rabbit purified polyclonal antibody)	This paper	RRID : AB_2722566	GeneCust compagny; rabbit purified polyclonal antibody; against CKFAGF(pT)FVDES AIDE; (1:2500)
antibody	anti-Sch9Total (rabbit polyclonal)	(Prouteau et al., 2017)		(1:20000)
antibody	anti-mouse IgG (whole Ab), HRP conjugate (polyclonal)	GE Healthcare	NA931 ; RRID : AB_772210	(1:10000)
antibody	anti-rabbit IgG (whole Ab), HRP conjugate (polyclonal)	GE Healthcare	NA934 ; RRID : AB_772206	(1:10000)
commercial assay or kit	Glucose Assay Kit	Sigma-Aldrich	GAGO20	Manufacture instructions
chemical compound, drug	R-5000 Rapamycin	LC Laoratories	53123-88-9	200 ng/ml
chemical compound, drug	CellTracker™ Blue CMAC Dye	Life technologies	C2110	
chemical compound, drug	Lumi-LightPlus Western blotting substrate	Roche	12015196001	Manufacture instructions
chemical compound, drug	Digitonin	Sigma-Aldrich	D141	

chemical compound, drug	Carbonyl cyanide 4-(trifluoromethoxy)phenylhydrazone (FCCP)	Sigma-Aldrich	C2920	20 µM
chemical compound, drug	Concanamycin A (Folimycin)	Abcam	ab144227	1 µM
chemical compound, drug	Bafilomycin A1	Cell Signaling TECHNOLOGY	54645S	1 µM
chemical compound, drug	Alanine, β-[1-14C]	Hartmann analytic	ARC0183	
chemical compound, drug	Arginine, L-[14C(U)]	Perkin-Elmer	NEC267E2	
chemical compound, drug	Leucine, L-[14C(U)]	Perkin-Elmer	NEC279E0	
chemical compound, drug	Glutamine, L-[14C(U)]	Perkin-Elmer	NEC4510	
chemical compound, drug	Fructose, D-[14C(U)]	Hartmann analytic	ARC0116	
software, algorithm	GraphPad Prism 5		RRID:SCR_015807	Statistical analysis and graphs representation

Yeast strains, plasmids, and growth conditions. The yeast strains used in this study (Table 1) derive from the Σ1278b wild type, the only exceptions being YPS14-4 (W303), JW00035 (W303), CEN.PK2-1c (VW1A), EBY.VW 4000, and I3. Cells were grown at 29°C on a minimal medium buffered at pH 6.1 (Jacobs et al., 1980), with glucose (Gluc) (3% w/v), maltose (3% w/v), galactose (Gal) (3% w/v), or ethanol (EtOH) (1% v/v) as a carbon source. For cultures in Gal medium, a low concentration of Gluc (0.3% w/v) was also added to boost initiation of growth. The nitrogen (N) sources added to liquid growth media were NH_4^+ as $(NH_4)_2SO_4$ (20 mM), proline (Pro) (10 mM), or urea (10 mM). For strain YPS14-4 and its derivative expressing *PMA4*$^{882\text{-}ochre}$, cells were grown on the same buffered minimal medium adjusted to pH 6.5 to improve growth. In all experiments, cells were examined or collected during exponential growth, a significant and regular number of generations after seeding. Our experience is that these precautions and the use of a minimal medium that is buffered considerably improve the reproducibility of data between biological replicates (Wiame et al., 1985). When indicated, rapamycin (Rap) at 200 ng/ml concentration was added for 30 min. The *ura3* mutation present in all strains was complemented by transformation with a plasmid, e. g. pFL38. Comparative analyses of growth were performed by growing cells in a Greiner 24-well microplate incubator coupled to a SYNERGY™ multi-mode reader (BioTek Instruments). The plasmids used in this study are listed in Table 2.

Fluorescence microscopy. Growing cells were laid on a thin layer of 1% agarose and viewed at room temperature with a fluorescence microscope (Eclipse E600; Nikon) equipped with a 100 differential interference contrast, numerical aperture (NA) 1.40 Plan-Apochromat objective (Nikon) and appropriate fluorescence light filter sets. Images were captured with a digital camera (DXM1200; Nikon) and ACT-1 acquisition software (Nikon) and processed with Photoshop CS (Adobe Systems). In each figure, we typically show only a few cells, representative of the whole population. Labeling

of the vacuolar membrane with CMAC fluorescent dye was performed by adding 1 µl of the dye to 5 ml of culture at least 30 min prior to visualization.

Protein extracts and western blotting. For western blot analysis, crude cell extracts were prepared as previously described (Hein et al., 1995). Proteins were transferred to a nitrocellulose membrane (Schleicher and Schuell; catalog number NBA085B) and probed with mouse anti-GFP (Roche; catalog number 11 814 460 001), anti-hemagglutinin (anti-HA) (12CA5; Roche), or anti-yeast 3-phosphoglycerate kinase (anti-PGK) (Invitrogen) or with rabbit anti-Pma1 (De Craene et al., 2001), anti-phospho-Thr^{737}-Sch9, or anti-$Sch9_{Total}$ (see below). Primary antibodies were detected with horseradish-peroxidase-conjugated anti-mouse or anti-rabbit immunoglobulin G secondary antibodies (GE Healthcare), followed by enhanced chemiluminescence (Roche; catalog number 12 015 196 001). Each Western blot was carried 2 to 4 times, a representative experiment is presented.

Generation and validation of the anti-phospho-Thr737-Sch9 antibody. The antibody was produced by and purchased from the GeneCust company. The CKFAGF(pT)FVDESAID peptide containing phosphorylated Thr737 was injected into rabbit. The affinity of the antibody preparation was tested in an ELISA for the phosphorylated peptide. Antibody specificity was tested by western blot analysis of cell extracts isolated from proline-grown wild-type (w-t) and *sch9Δ* strains, before and after addition of NH_4^+, well known to stimulate Sch9 phosphorylation (Fig. 1-figure supplement 2). The anti-$Sch9_{Total}$ antibody was a kind gift of Robbie Loewith.

Measurements of cytosolic pH. Yeast strains expressing a single *pHluorin* gene integrated into the genome or containing a multicopy plasmid expressing the *pHluorin* gene were grown at 29°C on Gluc proline buffered medium, pH 6.1, to OD660~0.2. Fluorescence intensities were recorded with a SYNERGY™ multi-mode microplate reader (BioTek Instruments) with emission filter 512/9 nm and excitation filters 395/9 and 475/9 nm, as previously reported (Orij et al., 2009; Zimmermannova et al., 2015). To eliminate the background fluorescence, pHluorin-nonproducing wild-type cells were grown in parallel, and the corresponding values at each excitation wavelength were subtracted from those of pHluorin-producing cells. The I395 nm to I475 nm emission intensity ratio was used to calculate the cytosolic pH. The fluorescence intensities of each strain were typically recorded in four separate cultures (1 ml culture per well) within one experiment (technical replicates), and the presented data are means ± SD of at least two independent experiments (biological replicates). The calibration curve was generated as described previously (Orij et al., 2009; Zimmermannova et al., 2015), with minor changes. The cell culture (100 ml, OD660 = 0.2) was filtered, washed, resuspended in 8 ml phosphate-buffered saline (Sigma) containing digitonin (175 µg/ml), and incubated for 15 min at RT. Digitonin was washed out and the cells were resuspended in 8 ml PBS (the OD of the cell suspension was about 2.5) and placed on ice. Then 40-µl aliquots were transferred to CELLSTAR black polystyrene clear-bottom 96-well microtiter plates (Greiner Bio-One) containing, per well, 160 µl citric acid/Na2HPO4 buffer at a pH ranging from 5.6 to 7.6 (in this volume, the OD was 0.5). Recording of pHluorin fluorescence emission and background subtraction were performed as

described above. The I395 nm to I475 nm intensity ratio was calculated, plotted against the corresponding buffer pH, and fitted to a third-degree polynomial regression curve.

Uptake measurements of radiolabelled compounds. The accumulation of [^{14}C]-labeled amino acids or [^{14}C]-labeled-fructose was measured at the time points indicated as previously described (Ghaddar et al., 2014a; Grenson et al., 1966). The radiolabeled compounds were purchased either from Perkin-Elmer or from Hartmann analytic. Data points represent averages of two biological replicates; error bars represent standard deviations (SD).

Measurement of total amino acid pools. Yeast cultures (50 ml) were collected by centrifugation (7000 g for 3 min) and washed twice with 10 ml Milli-Q water. The final pellet was resuspended in 2 ml Milli-Q water and boiled for 15 min. To remove cell debris, suspensions were centrifuged at 13 000 g for 1 min and filtered (Millipore 0.45 μm). The resulting soluble fractions were subjected to amino acid analysis after AccQ Tag pre-column derivatization (Waters). For this an AccQ Tag Ultra UPLC column (Waters) with UV detection at 260 nm was used according to the manufacturer's recommendations (Fayyad-Kazan et al., 2016).

Assay of trehalase activity in N-deprived cells. Cells growing on Gluc NH_4^+ medium were collected by filtration, and after washing and resuspension in Gluc medium without any N source, they were incubated overnight at 29°C with shaking. Cells were filtered, washed, and transferred again to fresh N-free Gluc medium for 30 min before addition of FCCP (20 μM). Culture samples were collected at various times and trehalase activity was measured in permeabilized cells as previously described (De Virgilio et al., 1991). Glucose levels were measured using the "Glucose assay kit" (Sigma-Aldrich).

Acknowledgements

We are grateful to Pierre Morsomme, Marc Boutry, Olga Zimmermannova, Hana Sychrova, Paula Gonçalves, Joris Winderickx, Wolf Frommer, Daniel Wipf, and Eckhard Boles for strains and plasmids, and Robbie Loewith for the antibody against Sch9. We also thank Catherine Jauniaux, Charlotte Felten, and Elizabeth Bodo for skillful technical assistance, Pierre Morsomme, Marc Boutry, and all lab members for fruitful discussions, and Eckhard Boles for advices about the experiments using the *hxt* null strain. E. Saliba is a fellow of the Fonds pour la Formation à la Recherche dans l'Industrie et l'Agriculture (FRIA). C. Gournas and M. Evangelinos are postdoctoral researchers of the Fonds de la Recherche Scientifique (F.R.S-FNRS). This work was supported by an FNRS grant (3.4.592.08.F) and the Algotech program of the Fédération Wallonie Bruxelles.

Competing interests

The authors declare that no competing interests exist.

References

Andersen, G., Andersen, B., Dobritzsch, D., Schnackerz, K.D., and Piskur, J. (2007). A gene duplication led to specialized gamma-aminobutyrate and beta-alanine aminotransferase in yeast. Febs J. *274*, 1804–1817.

Boeckstaens, M., Llinares, E., Van Vooren, P., and Marini, A.M. (2014). The TORC1 effector kinase Npr1 fine tunes the inherent activity of the Mep2 ammonium transport protein. Nat Commun *5*, 3101.

Boeckstaens, M., Merhi, A., Llinares, E., Van Vooren, P., Springael, J.Y., Wintjens, R., and Marini, A.M. (2015). Identification of a Novel Regulatory Mechanism of Nutrient Transport Controlled by TORC1-Npr1-Amu1/Par32. PLoS Genet. *11*, e1005382.

Bonfils, G., Jaquenoud, M., Bontron, S., Ostrowicz, C., Ungermann, C., and De Virgilio, C. (2012). Leucyl-tRNA Synthetase Controls TORC1 via the EGO Complex. Mol. Cell *46*, 105–110.

Bonneaud, N., Ozier-Kalogeropoulos, O., Li, G.Y., Labouesse, M., Minvielle-Sebastia, L., and Lacroute, F. (1991). A family of low and high copy replicative, integrative and single-stranded *S. cerevisiae*/*E. coli* shuttle vectors. Yeast *7*, 609–615.

Crapeau, M., Merhi, A., and André, B. (2014). Stress conditions promote yeast Gap1 permease ubiquitylation and down-regulation via the arrestin-like Bul and Aly proteins. J. Biol. Chem. *289*, 22103–22116.

Crespo, J.L., Powers, T., Fowler, B., and Hall, M.N. (2002). The TOR-controlled transcription activators GLN3, RTG1, and RTG3 are regulated in response to intracellular levels of glutamine. Proc. Natl. Acad. Sci. U.S.a. *99*, 6784–6789.

Cui, X., and Xie, Z. (2017). Protein Interaction and Na/K-ATPase-Mediated Signal Transduction. Molecules *22*, 990.

De Craene, J.O., Soetens, O., and André, B. (2001). The Npr1 kinase controls biosynthetic and endocytic sorting of the yeast Gap1 permease. J. Biol. Chem. *276*, 43939–43948.

De Virgilio, C., Bürckert, N., Boller, T., and Wiemken, A. (1991). A method to study the rapid phosphorylation-related modulation of neutral trehalase activity by temperature shifts in yeast. FEBS Lett. *291*, 355–358.

Dechant, R., Saad, S., Ibáñez, A.J., and Peter, M. (2014). Cytosolic pH regulates cell growth through distinct GTPases, Arf1 and Gtr1, to promote Ras/PKA and TORC1 activity. Mol. Cell *55*, 409–421.

Donaton, M.C.V., Holsbeeks, I., Lagatie, O., Van Zeebroeck, G., Crauwels, M., Winderickx, J., and Thevelein, J.M. (2003). The Gap1 general amino acid permease acts as an amino acid sensor for activation of protein kinase A targets in the yeast *Saccharomyces cerevisiae*. Mol. Microbiol. *50*, 911–929.

793 Dubouloz, F., Deloche, O., Wanke, V., Cameroni, E., and De Virgilio, C. (2005). The
794 TOR and EGO protein complexes orchestrate microautophagy in yeast. Mol. Cell *19*,
795 15–26.

796 Durán, R.V., and Hall, M.N. (2012). Regulation of TOR by small GTPases. EMBO Rep.
797 *13*, 121–128.

798 Eltschinger, S., and Loewith, R. (2016). TOR Complexes and the Maintenance of
799 Cellular Homeostasis. Trends Cell Biol. *26*, 148–159.

800 Eraso, P., and Gancedo, C. (1987). Activation of yeast plasma membrane ATPase by
801 acid pH during growth. FEBS Lett. *224*, 187–192.

802 Fayyad-Kazan, M., Feller, A., Bodo, E., Boeckstaens, M., Marini, A.M., Dubois, E., and
803 Georis, I. (2016). Yeast Nitrogen Catabolite Repression is sustained by signals distinct
804 from glutamine and glutamate reservoirs. Mol. Microbiol. *99*, 360–379.

805 Galeote, V., Novo, M., Salema-Oom, M., Brion, C., Valério, E., Gonçalves, P., and
806 Dequin, S. (2010). FSY1, a horizontally transferred gene in the Saccharomyces
807 cerevisiae EC1118 wine yeast strain, encodes a high-affinity fructose/H+ symporter.
808 Microbiology *156*, 3754–3761.

809 Gao, M., and Kaiser, C.A. (2006). A conserved GTPase-containing complex is required
810 for intracellular sorting of the general amino-acid permease in yeast. Nat. Cell Biol. *8*,
811 657–667.

812 Ghaddar, K., Krammer, E.-M., Mihajlovic, N., Brohée, S., André, B., and Prévost, M.
813 (2014a). Converting the yeast arginine Can1 permease to a lysine permease. J. Biol.
814 Chem. *289*, 7232–7246.

815 Ghaddar, K., Merhi, A., Saliba, E., Krammer, E.-M., Prévost, M., and André, B.
816 (2014b). Substrate-induced ubiquitylation and endocytosis of yeast amino Acid
817 permeases. Mol. Cell. Biol. *34*, 4447–4463.

818 Goberdhan, D.C.I., Wilson, C., and Harris, A.L. (2016). Amino Acid Sensing by
819 mTORC1: Intracellular Transporters Mark the Spot. Cell Metab. *23*, 580–589.

820 González, A., and Hall, M.N. (2017). Nutrient sensing and TOR signaling in yeast and
821 mammals. Embo J. *36*, 397–408.

822 Gournas, C., Evangelidis, T., Athanasopoulos, A., Mikros, E., and Sophianopoulou, V.
823 (2015). The Aspergillus nidulans proline permease as a model for understanding the
824 factors determining substrate binding and specificity of fungal amino acid
825 transporters. J. Biol. Chem. *290*, 6141–6155.

826 Gournas, C., Prévost, M., Krammer, E.-M., and André, B. (2016). Function and
827 Regulation of Fungal Amino Acid Transporters: Insights from Predicted Structure.
828 Adv. Exp. Med. Biol. *892*, 69–106.

829 Gournas, C., Saliba, E., Krammer, E.-M., Barthélemy, C., Prévost, M., and André, B.

(2017). Transition of yeast Can1 transporter to the inward-facing state unveils an α-arrestin target sequence promoting its ubiquitylation and endocytosis. Mol. Biol. Cell mbc.E17–02–0104.

Grenson, M., Mousset, M., Wiame, J.M., and Béchet, J. (1966). Multiplicity of the amino acid permeases in *Saccharomyces cerevisiae*. I. Evidence for a specific arginine-transporting system. Biochim. Biophys. Acta *127*, 325–338.

Han, J.M., Jeong, S.J., Park, M.C., Kim, G., Kwon, N.H., Kim, H.K., Ha, S.H., Ryu, S.H., and Kim, S. (2012). Leucyl-tRNA Synthetase Is an Intracellular Leucine Sensor for the mTORC1-Signaling Pathway. Cell *149*, 410–424.

Hatakeyama, R., and De Virgilio, C. (2016). Unsolved mysteries of Rag GTPase signaling in yeast. Small GTPases *7*, 239–246.

Hein, C., and André, B. (1997). A C-terminal di-leucine motif and nearby sequences are required for NH4(+)-induced inactivation and degradation of the general amino acid permease, Gap1p, of *Saccharomyces cerevisiae*. Mol. Microbiol. *24*, 607–616.

Hein, C., Springael, J.Y., Volland, C., Haguenauer-Tsapis, R., and André, B. (1995). *NPI1*, an essential yeast gene involved in induced degradation of Gap1 and Fur4 permeases, encodes the Rsp5 ubiquitin-protein ligase. Mol. Microbiol. *18*, 77–87.

Heitman, J., Movva, N.R., and Hall, M.N. (1991). Targets for cell cycle arrest by the immunosuppressant rapamycin in yeast. Science *253*, 905–909.

Hughes Hallett, J.E., Luo, X., and Capaldi, A.P. (2014). State Transitions in the TORC1 Signaling Pathway and Information Processing in Saccharomyces cerevisiae. Genetics *198*, 773–786.

Hughes Hallett, J.E., Luo, X., and Capaldi, A.P. (2015). Snf1/AMPK promotes the formation of Kog1/Raptor-bodies to increase the activation threshold of TORC1 in budding yeast. Elife *4*, e09181.

Jacobs, P., Jauniaux, J.C., and Grenson, M. (1980). A cis-dominant regulatory mutation linked to the argB-argC gene cluster in Saccharomyces cerevisiae. J. Mol. Biol. *139*, 691–704.

Jewell, J.L., Kim, Y.C., Russell, R.C., Yu, F.-X., Park, H.W., Plouffe, S.W., Tagliabracci, V.S., and Guan, K.-L. (2015). Metabolism. Differential regulation of mTORC1 by leucine and glutamine. Science *347*, 194–198.

Kane, P.M. (2016). Proton Transport and pH Control in Fungi. Adv. Exp. Med. Biol. *892*, 33–68.

Kim, A., and Cunningham, K.W. (2015). A LAPF/phafin1-like protein regulates TORC1 and lysosomal membrane permeabilization in response to endoplasmic reticulum membrane stress. Mol. Biol. Cell *26*, 4631–4645.

Kim, E., Goraksha-Hicks, P., Li, L., Neufeld, T.P., and Guan, K.-L. (2008). Regulation of

867 TORC1 by Rag GTPases in nutrient response. Nat. Cell Biol. *10*, 935–945.

868 Lai, F., Madan, N., Ye, Q., Duan, Q., Li, Z., Wang, S., Si, S., and Xie, Z. (2013).
869 Identification of a mutant α1 Na/K-ATPase that pumps but is defective in signal
870 transduction. J. Biol. Chem. *288*, 13295–13304.

871 Lauwers, E., and André, B. (2006). Association of yeast transporters with detergent-
872 resistant membranes correlates with their cell-surface location. Traffic *7*, 1045–1059.

873 Loewith, R., and Hall, M.N. (2011). Target of rapamycin (TOR) in nutrient signaling
874 and growth control. Genetics *189*, 1177–1201.

875 Luo, H., Morsomme, P., and Boutry, M. (1999). The two major types of plant plasma
876 membrane H+-ATPases show different enzymatic properties and confer differential
877 pH sensitivity of yeast growth. Plant Physiol. *119*, 627–634.

878 MacGurn, J.A., Hsu, P.-C., Smolka, M.B., and Emr, S.D. (2011). TORC1 regulates
879 endocytosis via Npr1-mediated phosphoinhibition of a ubiquitin ligase adaptor. Cell
880 *147*, 1104–1117.

881 Mahmoud, S., Planes, M.D., Cabedo, M., Trujillo, C., Rienzo, A., Caballero-Molada,
882 M., Sharma, S.C., Montesinos, C., Mulet, J.M., and Serrano, R. (2017). TOR complex 1
883 regulates the yeast plasma membrane proton pump and pH and potassium
884 homeostasis. FEBS Lett. *591*, 1993–2002.

885 Merhi, A., and André, B. (2012). Internal amino acids promote Gap1 permease
886 ubiquitylation via TORC1/Npr1/14-3-3-dependent control of the Bul arrestin-like
887 adaptors. Mol. Cell. Biol. *32*, 4510–4522.

888 Merhi, A., Gérard, N., Lauwers, E., Prévost, M., and André, B. (2011). Systematic
889 mutational analysis of the intracellular regions of yeast Gap1 permease. PLoS ONE *6*,
890 e18457.

891 Morsomme, P., Slayman, C.W., and Goffeau, A. (2000). Mutagenic study of the
892 structure, function and biogenesis of the yeast plasma membrane H(+)-ATPase.
893 Biochim. Biophys. Acta *1469*, 133–157.

894 Mumberg, D., Müller, R., and Funk, M. (1994). Regulatable promoters of
895 *Saccharomyces cerevisiae*: comparison of transcriptional activity and their use for
896 heterologous expression. Nucleic Acids Res. *22*, 5767–5768.

897 Nikko, E., Marini, A.M., and André, B. (2003). Permease recycling and ubiquitination
898 status reveal a particular role for Bro1 in the multivesicular body pathway. J. Biol.
899 Chem. *278*, 50732–50743.

900 Orij, R., Postmus, J., Beek, Ter, A., Brul, S., and Smits, G.J. (2009). In vivo
901 measurement of cytosolic and mitochondrial pH using a pH-sensitive GFP derivative
902 in Saccharomyces cerevisiae reveals a relation between intracellular pH and growth.
903 Microbiology (Reading, Engl.) *155*, 268–278.

Orij, R., Urbanus, M.L., Vizeacoumar, F.J., Giaever, G., Boone, C., Nislow, C., Brul, S., and Smits, G.J. (2012). Genome-wide analysis of intracellular pH reveals quantitative control of cell division rate by pH(c) in Saccharomyces cerevisiae. Genome Biol. *13*, R80.

Palmgren, M.G., and Christensen, G. (1994). Functional comparisons between plant plasma membrane H(+)-ATPase isoforms expressed in yeast. J. Biol. Chem. *269*, 3027–3033.

Panchaud, N., Péli-Gulli, M.-P., and De Virgilio, C. (2013a). Amino Acid Deprivation Inhibits TORC1 Through a GTPase-Activating Protein Complex for the Rag Family GTPase Gtr1. Sci Signal *6*, ra42.

Panchaud, N., Péli-Gulli, M.-P., and De Virgilio, C. (2013b). SEACing the GAP that nEGOCiates TORC1 activation: evolutionary conservation of Rag GTPase regulation. Cell Cycle *12*, 2948–2952.

Pinson, B., Napias, C., Chevallier, J., Van den Broek, P.J., and Bréthes, D. (1997). Characterization of the Saccharomyces cerevisiae cytosine transporter using energizable plasma membrane vesicles. J. Biol. Chem. *272*, 28918–28924.

Portillo, F. (2000). Regulation of plasma membrane H(+)-ATPase in fungi and plants. Biochim. Biophys. Acta *1469*, 31–42.

Portillo, F., de Larrinoa, I.F., and Serrano, R. (1989). Deletion analysis of yeast plasma membrane H+-ATPase and identification of a regulatory domain at the carboxyl-terminus. FEBS Lett. *247*, 381–385.

Powis, K., and De Virgilio, C. (2016). Conserved regulators of Rag GTPases orchestrate amino acid-dependent TORC1 signaling. Cell Discov *2*, 15049.

Prouteau, M., Desfosses, A., Sieben, C., Bourgoint, C., Lydia Mozaffari, N., Demurtas, D., Mitra, A.K., Guichard, P., Manley, S., and Loewith, R. (2017). TORC1 organized in inhibited domains (TOROIDs) regulate TORC1 activity. Nature *550*, 265–269.

Rodrigues de Sousa, H., Spencer-Martins, I., and Gonçalves, P. (2004). Differential regulation by glucose and fructose of a gene encoding a specific fructose/H+ symporter in Saccharomyces sensu stricto yeasts. Yeast *21*, 519–530.

Sancak, Y., Bar-Peled, L., Zoncu, R., Markhard, A.L., Nada, S., and Sabatini, D.M. (2010). Ragulator-Rag complex targets mTORC1 to the lysosomal surface and is necessary for its activation by amino acids. Cell *141*, 290–303.

Sancak, Y., Peterson, T.R., Shaul, Y.D., Lindquist, R.A., Thoreen, C.C., Bar-Peled, L., and Sabatini, D.M. (2008). The Rag GTPases bind raptor and mediate amino acid signaling to mTORC1. Science *320*, 1496–1501.

Saxton, R.A., and Sabatini, D.M. (2017). mTOR Signaling in Growth, Metabolism, and Disease. Cell *168*, 960–976.

941 Schmidt, A., Beck, T., Koller, A., Kunz, J., and Hall, M.N. (1998). The TOR nutrient
942 signalling pathway phosphorylates NPR1 and inhibits turnover of the tryptophan
943 permease. Embo J. *17*, 6924–6931.

944 Schothorst, J., Kankipati, H.N., Conrad, M., Samyn, D.R., Van Zeebroeck, G., Popova,
945 Y., Rubio-Texeira, M., Persson, B.L., and Thevelein, J.M. (2013). Yeast nutrient
946 transceptors provide novel insight in the functionality of membrane transporters.
947 Curr. Genet. *59*, 197–206.

948 Serrano, R. (1983). In vivo glucose activation of the yeast plasma membrane ATPase.
949 FEBS Lett. *156*, 11–14.

950 Stolz, J., and Sauer, N. (1999). The fenpropimorph resistance gene FEN2 from
951 Saccharomyces cerevisiae encodes a plasma membrane H+-pantothenate
952 symporter. J. Biol. Chem. *274*, 18747–18752.

953 Stracka, D., Jozefczuk, S., Rudroff, F., Sauer, U., and Hall, M.N. (2014). Nitrogen
954 Source Activates TOR Complex 1 via Glutamine and Independently of Gtr/Rag. J. Biol.
955 Chem. *289*, 25010–25020.

956 Supply, P., Wach, A., Thinès-Sempoux, D., and Goffeau, A. (1993). Proliferation of
957 intracellular structures upon overexpression of the PMA2 ATPase in Saccharomyces
958 cerevisiae. J. Biol. Chem. *268*, 19744–19752.

959 Tanigawa, M., and Maeda, T. (2017). An In Vitro TORC1 Kinase Assay That
960 Recapitulates the Gtr-Independent Glutamine-Responsive TORC1 Activation
961 Mechanism on Yeast Vacuoles. Mol. Cell. Biol. *37*, e00075–17.

962 Ullah, A., Orij, R., Brul, S., and Smits, G.J. (2012). Quantitative analysis of the modes
963 of growth inhibition by weak organic acids in Saccharomyces cerevisiae. Appl.
964 Environ. Microbiol. *78*, 8377–8387.

965 Urban, J., Soulard, A., Huber, A., Lippman, S., Mukhopadhyay, D., Deloche, O.,
966 Wanke, V., Anrather, D., Ammerer, G., Riezman, H., et al. (2007). Sch9 is a major
967 target of TORC1 in Saccharomyces cerevisiae. Mol. Cell *26*, 663–674.

968 Varlakhanova, N.V., Mihalevic, M.J., Bernstein, K.A., and Ford, M.G.J. (2017). Pib2
969 and the EGO complex are both required for activation of TORC1. J Cell Sci *130*, 3878–
970 3890.

971 Wiame, J.M., Grenson, M., and Arst, H.N. (1985). Nitrogen catabolite repression in
972 yeasts and filamentous fungi. Adv. Microb. Physiol. *26*, 1–88.

973 Wieczorke, R., Krampe, S., Weierstall, T., Freidel, K., Hollenberg, C.P., and Boles, E.
974 (1999). Concurrent knock-out of at least 20 transporter genes is required to block
975 uptake of hexoses in Saccharomyces cerevisiae. FEBS Lett. *464*, 123–128.

976 Wilms, T., Swinnen, E., Eskes, E., Dolz-Edo, L., Uwineza, A., Van Essche, R., Rosseels,
977 J., Zabrocki, P., Cameroni, E., Franssens, V., et al. (2017). The yeast protein kinase

978 Sch9 adjusts V-ATPase assembly/disassembly to control pH homeostasis and
979 longevity in response to glucose availability. PLoS Genet. *13*, e1006835.

980 Wipf, D., Benjdia, M., Tegeder, M., and Frommer, W.B. (2002). Characterization of a
981 general amino acid permease from Hebeloma cylindrosporum. FEBS Lett. *528*, 119–
982 124.

983 Wolfson, R.L., and Sabatini, D.M. (2017). The Dawn of the Age of Amino Acid Sensors
984 for the mTORC1 Pathway. Cell Metab. *26*, 301–309.

985 Zheng, X., Liang, Y., He, Q., Yao, R., Bao, W., Bao, L., Wang, Y., and Wang, Z. (2014).
986 Current models of mammalian target of rapamycin complex 1 (mTORC1) activation
987 by growth factors and amino acids. Int J Mol Sci *15*, 20753–20769.

988 Zimmermannova, O., Salazar, A., Sychrova, H., and Ramos, J. (2015).
989 Zygosaccharomyces rouxii Trk1 is an efficient potassium transporter providing yeast
990 cells with high lithium tolerance. FEMS Yeast Res. *15*, fov029.

991 Zoncu, R., Bar-Peled, L., Efeyan, A., Wang, S., Sancak, Y., and Sabatini, D.M. (2011).
992 mTORC1 senses lysosomal amino acids through an inside-out mechanism that
993 requires the vacuolar H(+)-ATPase. Science *334*, 678–683.

994

995

996

Table 1. Yeast strains used in this study

Strain	Genotype	Reference or source
23344c	*ura3*	Laboratory collection
EK008	*gap1Δ ura3*	Lab collection
ES032	*can1Δ ura3*	(Gournas et al., 2017)
ES029	*gap1Δ can1Δ ura3*	(Gournas et al., 2017)
MA032	*gap1Δ BUL2-HA ura3*	(Merhi and André, 2012)
27038a	*npi1-1^{rsp5} ura3*	(Hein et al., 1995)
OS27-1	*bul1Δ bul2Δ ura3*	Lab collection
34210c	*gap1Δ put4Δ ura3*	Lab collection
33007c	*gap1Δ ura3 leu2*	Lab collection
30911b	*car1 ura3*	Lab collection
CG059	*gap1Δ can1Δ ura3 leu2*	(Gournas et al., 2017)
OS26-1	*gtr1Δ gtr2Δ ura3*	Lab collection
CEN.PK2-1c	*leu2-3,112 ura3-52 trp1-289 his3-Δ1 MAL2-8c SUC2 hxt17Δ*	(Wieczorke et al., 1999)
EBY.VW4000	*hxt1-17Δ gal2Δ stl1Δ agt1Δ mph2Δ mph3Δ leu2-3,112 ura3-52 trp1-289 his3-Δ1 MAL2-8c SUC2*	(Wieczorke et al., 1999)
I3	*EBY.VW4000 URA3::FSY1*	(Rodrigues de Sousa et al., 2004)
CG146	*seh1Δ ura3*	This study
CG148	*pib2Δ ura3*	This study
CG150	*iml1Δ ura3*	This study
35652d	*fcy1 ura3*	This study
ES075	*uga1::loxP-kanMX-loxP-GPD1p-pHluorin ura3*	This study
YPS14-4	*ade 2–101, leu2Δ1, his3-Δ200, ura3–52, trp1Δ63, lys2–801 pma1Δ::HIS3, pma2Δ::TRP1 + YCp-(Sc)PMA1 (LEU2)*	(Supply et al., 1993)
PMA4-882Ochre	*ade 2–101, leu2Δ1, his3-Δ200, ura3–52, trp1Δ63, lys2–801 pma1Δ::HIS3, pma2Δ::TRP1 + YEp-PMA1p-(Np)PMA4^{882ochre} (LEU2)*	(Luo et al., 1999)
JW00035	*leu2-3-112 ura3-1 trp1-1 his3-11-15 ade2-1 can1-100 sch9Δ::TRP1*	(Wilms et al., 2017)
JX023	*GAL1p-PMA1 pma2Δ ura3 leu2*	This study

997

Table 2. Plasmids used in this study

Plasmid	Description	Reference or source
pFL38	CEN-ARS (URA3)	(Bonneaud et al., 1991)
pFL36	CEN-ARS (LEU2)	(Bonneaud et al., 1991)
p416 GAL1	CEN-ARS GAL1p (URA3)	(Mumberg et al., 1994)
pJOD10	p416 GAL1p-GAP1-GFP (URA3)	(Nikko et al., 2003)
pCJ038	p416 GAL1p -GAP1(K9R,K16R)-GFP (URA3)	(Lauwers and André, 2006)
pMA065	p416 GAL1p -GAP1-126-GFP (URA3)	(Merhi et al., 2011)
pMA091	p416 GAL1p -GAP1-126-K9R,K16R-GFP (URA3)	(Merhi et al., 2011)
pCH500	CEN-ARS-GAP1 (URA3)	(Hein and André, 1997)
pHcGAP1	YEp-HcGAP1 (URA3)	(Wipf et al., 2002)
pES103	YEp-HA-NPR1 (LEU2)	This study
pAS103	YEp-HA-NPR1 (URA3)	(Schmidt et al., 1998)
pCJ315	CEN-ARS (LEU2-HIS3-LYS2)	Lab collection
pMYC008	YCp-AGP1p-LACZ (HIS3 TRP1 LEU2)	Lab collection
pES154	YCp-AGP1p-LACZ (HIS3 TRP1)	This study
pHl-U	YEp-ADH1p-pHluorin (URA3)	(Orij et al., 2009; Zimmermannova et al., 2015)
pHl-I	YCp-loxP-kanMX-loxP-GPD1p-pHluorin (URA3)	(Orij et al., 2009; Zimmermannova et al., 2015)
pCJ366	YEp (TRP1-LEU2-HIS3)	Lab collection
pPS15-P1	YCp-(Sc)PMA1 (LEU2)	(Supply et al., 1993)
pPMA4882ochre	YEp-PMA1p-(Np)PMA4^{882ochre} (LEU2)	(Luo et al., 1999)

998

999

Figure legends

Figure 1. Uptake of β-alanine via the Gap1 permease causes Rag/Gtr-dependent TORC1 activation without increasing the internal pools of amino acids (A) Top. Wild-type (w-t) and *gap1Δ* cells were grown on Gluc Pro medium and [^{14}C]-β-ala (0.5 mM) was added to the medium before measurement of the incorporated radioactivity at various times. Bottom. w-t cells were grown for 4 days on solid minimal medium without any N source or with GABA (0.5 mM) or β-ala (0.5 mM) as sole N source. **(B)** *gap1Δ* cells expressing, from plasmids, a gene encoding GFP-fused Gap1, Gap1(K9R-K16R), or Gap1-126 were grown on Gal Pro medium. Glucose was added for 30 min to stop Gap1 neosynthesis prior to addition of β-ala (0.5 mM) for 4 min. Crude cell extracts were prepared and immunoblotted with anti-GFP and anti-Pma1 antibodies. **(C)** Fluorescence microscopy analysis of the cells in 1B. Cells were grown on Gal Pro medium. Glucose was added for 1.5 h to stop Gap1 neosynthesis, and β-ala (0.5 mM) was added for 30 min or 1 h. CMAC staining (blue) was used to highlight the vacuole. **(D)** Top. w-t and *gap1Δ* cells expressing HA-Npr1 from a plasmid were grown on Gluc Pro medium. Cells were collected before and at various times after addition of β-ala (0.5 mM). Crude extracts were prepared and immunoblotted with anti-HA and anti-Pgk antibodies. Bottom. Same as in the top panel, except that w-t cells were collected before and 4 min after addition of β-ala (0.5 mM). Rap was added to half of the culture for 30 min, before addition of β-ala (0.5 mM). **(E)** Top. w-t and *gap1Δ* cells were grown on Gluc Pro medium. Cells were collected before and 4 and 10 min after addition of β-ala (0.5 mM). Crude extracts were prepared and immunoblotted with anti-(P) T^{737}-Sch9 and anti-$Sch9_{Total}$ antibodies. Bottom. Same as in panel G, except that w-t cells were collected before and 4 min after addition of β-ala (0.5 mM). Half of the culture was pretreated with Rap for 30 min. **(F)** w-t cells were grown on Gluc Pro medium. Cell extracts were prepared before and 30 min after addition of β-ala (0.5 mM) and used to measure amino acid pools as described under Materials and Methods. The presented data are means ± SD of two independent experiments. **(G)** w-t and *gtr1Δ gtr2Δ* cells expressing HA-Npr1 from a plasmid were grown on Gluc Pro medium. Cells were collected before and 4 and 10 min after addition of β-ala (0.5 mM). Crude extracts

were prepared and immunoblotted with anti-HA and anti-Pgk antibodies. **(H)** Cells as in G were grown on Gluc Pro medium. [^{14}C]-β-ala (0.5 mM) was added to the medium before measuring the incorporated radioactivity at various times.

Figure 2. Uptake of β-ala via the endogenous Put4 or the heterologous HcGap1 permease also promotes TORC1 activation (A) w-t, *gap1Δ*, and *gap1Δ put4Δ* cells were grown on Gluc urea medium. [^{14}C]-β-ala (0.1 or 2 mM) was added to the medium before measuring the incorporated radioactivity at various times. **(B)** Top. Cells as in A expressing HA-Npr1 from a plasmid were grown on Gluc urea medium. Cells were collected before and 4 and 10 min after addition of β-ala (0.1 or 2 mM). Crude extracts were prepared and immunoblotted with anti-HA and anti-Pgk antibodies. Bottom. Same as in panel B except that *gap1Δ* cells were also collected 30 min after Rap treatment. **(C)** w-t and *gap1Δ* cells expressing or not Hc-Gap1 from a plasmid were grown on Gluc Pro medium. [^{14}C]-β-ala (0.5 or 2 mM) was added to the medium before measuring the incorporated radioactivity at various times. **(D)** Top. w-t and *gap1Δ* cells expressing HA-Npr1 and *gap1Δ* cells co-expressing pHc-Gap1 and HA-Npr1 from plasmids were grown on Gluc Pro medium. Cells were collected before and 4 and 10 min after addition of β-ala (0.5 or 2 mM). Crude extracts were prepared and immunoblotted with anti-HA and anti-Pgk antibodies. Bottom. Same as in top panel except that cells were also treated for 30 min with Rap before β-ala addition.

Figure 3. Uptake of arginine via an endogenous or a heterologous permease stimulates TORC1 even if arginine catabolism is impaired. (A) Left. w-t, *gap1Δ*, *can1Δ*, and *gap1Δ can1Δ* cells were grown on Gluc Pro medium. [^{14}C]-L-Arg (0.5 mM) was added to the medium before measuring the incorporated radioactivity at various times. Right. Cells as in A expressing HA-Npr1 from a plasmid were grown on Gluc Pro medium and collected before and 4 and 10 min after addition of Arg (0.5 mM). Crude extracts were prepared and immunoblotted with anti-HA and anti-Pgk antibodies. **(B)** Left top. w-t and *gtr1Δ gtr2Δ* cells expressing HA-Npr1 from a plasmid were grown on Gluc Pro medium. Cells were collected before and 4 and 10 min after

addition of Arg (0.5 mM). Crude extracts were prepared and immunoblotted with anti-HA and anti-Pgk antibodies. Left bottom. Same as in panel left top except that half of the culture was treated for 30 min by Rap before addition of Arg. Right. Cells as in left panels though not expressing HA-Npr1 were grown on Gluc Pro medium. [^{14}C]-L-Arg (0.5 mM) was added to the medium before measuring the incorporated radioactivity at various times. **(C)** w-t cells were grown on Gluc Pro medium. Cells were collected before and 4 and 10 min after addition of Arg (0.5 mM). Crude extracts were prepared and immunoblotted with anti-(P) T^{737}-Sch9 and anti-Sch9$_{Total}$ antibodies. **(D)** w-t and *gap1Δ can1Δ* cells expressing or not Hc-GAP1 from a plasmid were grown on Gluc Pro medium. [^{14}C]-L-Arg (0.5 or 1 mM) was added to the medium before measurement of the incorporated radioactivity at various times. **(E)** Top. w-t and *gap1Δ can1Δ* cells expressing HA-Npr1 from plasmid, and *gap1Δ can1Δ* cells co-expressing Hc-GAP1 and HA-Npr1 from plasmids, were grown on Gluc Pro medium. Cells were collected before and 4 and 10 min after addition of Arg (0.5 or 1 mM). Crude extracts were prepared and immunoblotted with anti-HA and anti-Pgk antibodies. Bottom. Same as in top panel except that half of the culture was treated for 30 min with Rap before addition of Arg. **(F)** Left. w-t and *car1* mutant cells were grown on solid minimal medium with NH_4^+ or Arg at a concentration of 2 mM as sole N source. **(G)**. *car1* mutant cells expressing HA-Npr1 from a plasmid were grown on Gluc Pro medium. Cells were collected before and 4 and 10 min after addition of Arg (0.5 mM), and part of the culture was also treated for 30 min with Rap before Arg addition. Crude extracts were prepared and immunoblotted with anti-HA and anti-Pgk antibodies.

Figure 4. H^+ influx coupled to transport promotes Rag/Gtr-dependent stimulation of TORC1. (A) The β-ala uptake activities of Gap1 (in w-t cells grown on Gluc Pro medium), Put4 (in *gap1Δ* cells grown on Gluc urea medium), and Hc-Gap1 (in *gap1Δ* cells expressing Hc-Gap1 and grown on Gluc Pro medium), were determined by measuring the initial rate of [^{14}C]-β-ala incorporation (0.5 mM for Gap1, 2 mM for Put4 and Hc-Gap1) before and after glucose starvation for 5 min or with or without prior incubation with FCCP (20 µM) or its solvent (0.2 % EtOH) for 5 min. The presented data are means ± SD of two independent experiments. **(B)** The Arg uptake

activities of Gap1 and Can1 (in w-t cells), of Gap1 alone (in *can1Δ* cells), of Can1 alone (in *gap1Δ* cells), and of Hc-Gap1 (in *gap1Δ can1Δ* cells expressing Hc-Gap1 from a plasmid) were determined by measuring the initial rate of [^{14}C]-L-Arg incorporation (0.5 mM for Gap1 and Can1, 1 mM for Hc-Gap1) as in A. The presented data are means ± SD of two independent experiments. **(C)** w-t cells expressing HA-Npr1 from a plasmid were grown on Gluc Pro medium. Cells were collected 4 min after addition of cytosine (1 mM). Half of the culture was treated with Rap for 30 min before addition of cytosine. Crude extracts were prepared and immunoblotted with anti-HA and anti-Pgk antibodies. **(D)** w-t cells were grown on Gluc Pro medium. Cells were collected before and 4 and 10 min after addition of cytosine (1 mM). Crude extracts were prepared and immunoblotted with anti-(P) T^{737}-Sch9 and anti-$Sch9_{Total}$ antibodies. **(E)** w-t and *gtr1 gtr2Δ* cells expressing HA-Npr1 from a plasmid were grown on Gluc Pro medium. Cells were collected before and 4 and 10 min after addition of cytosine (1 mM). Crude extracts were prepared and immunoblotted with anti-HA and anti-Pgk antibodies. **(F)** Left. w-t and *fcy1* cells were grown on solid medium with NH_4^+ or cytosine (2 mM) as sole N source. Right. *fcy1* cells expressing HA-Npr1 were grown on Gluc Pro medium. Cells were collected before and 4 and 10 min after addition of cytosine (0.5 mM). Half of the culture was treated for 30 min with Rap before addition of cytosine. Crude extracts were prepared and immunoblotted with anti-HA and anti-Pgk antibodies. **(G)** w-t (CEN.PK2-1c), *hxtΔ* (EBY.VW4000), and *hxtΔ + FSY1* (I3) cells were grown on maltose NH_4^+ medium, shifted for 6h on EtOH Pro, and [^{14}C]-D-fructose (2 mM) was added to the medium before measuring the incorporated radioactivity at various times. **(H)** Cells of the w-t and *hxtΔ + FSY1* srains (as in G) were grown on maltose NH_4^+ medium. The initial rate of [^{14}C]-D-fructose incorporation (2 mM), with or without prior incubation with FCCP (20 µM) for 5 min, was then measured. The data are means ± SD of two independent experiments. **(I)** Strains and growth conditions as in G. Cells were collected before and 2, 4 and 10 min after addition of fructose (2 mM). For the I3 strain, half of the culture was treated for 30 min with Rap before addition of fructose. Crude extracts were prepared and immunoblotted with anti-(P) T^{737}-Sch9 and anti-$Sch9_{Total}$ antibodies.

Figure 5. H^+ diffusion via a protonophore promotes Rag/Gtr-dependent stimulation of TORC1 (A) w-t cells expressing pHluorin (strain ES075) were grown on Gluc Pro medium. The cytosolic pH was monitored for 30 min at regular intervals. FCCP (20 µM) or its solvent (0.2% EtOH) was added at 1 min. **(B)** w-t cells expressing HA-Npr1 from a plasmid were grown on Gluc Pro medium. Cells were collected before and at various times after addition of FCCP (20 µM) or its solvent (0.2% EtOH). Part of the culture was treated for 30 min with Rap before addition of FCCP. Crude extracts were prepared and immunoblotted with anti-HA and anti-Pgk antibodies. **(C)** w-t cells were grown on Gluc Pro medium. Cells were collected before and at various times after addition of FCCP (20 µM) or its solvent (0.2 % EtOH). Crude extracts were prepared and immunoblotted with anti-(P) T^{737}-Sch9 and anti-$Sch9_{Total}$ antibodies. **(D-G)** w-t and *gtr1 gtr2Δ, seh1Δ, iml1Δ* or *pib2Δ* cells expressing HA-Npr1 from a plasmid were grown on Gluc Pro medium. Cells were collected before and at various times after FCCP addition (20 µM). Crude extracts were prepared and immunoblotted with anti-HA and anti-Pgk antibodies.

Figure 6. Inhibition of the vacuolar V-ATPase activates TORC1. (A) w-t cells expressing pHluorin (strain ES075) were grown on Gluc Pro medium. The cytosolic pH was monitored for 30 min at regular intervals. Concanamycin A (CMA) (1 µM) or its solvent (0.2% EtOH) was added at 1 min. **(B)** Left. w-t cells expressing HA-Npr1 from a plasmid were grown on Gluc Pro medium. Cells were collected before and at various times after addition of CMA (1 µM) or its solvent (0.2% EtOH). Crude extracts were prepared and immunoblotted with anti-HA and anti-Pgk antibodies. Right. Same except that half of the culture was treated with Rap for 30 min before CMA addition. **(C)** Same as in B except that crude extracts from w-t cells were immunoblotted with anti-(P) T^{737}-Sch9 and anti-$Sch9_{Total}$ antibodies. **(D)** Same as in B except that w-t and *gtr1Δ gtr2Δ* cells were analyzed. **(E, F, G, H)** Same as in A, B, C and D, respectively, except that cells were treated with bafilomycin A (BAF) (1 µM). The data of Fig. 6A and 6E and those of Fig. 5A were obtained in the same experiments but are presented in separate graphs for clarity.

Figure 7. TORC1 activation in response to increased cytosolic H^+ involves the Pma1 H^+-ATPase. (A) *GAL1p-PMA1 pma2Δ* cells transformed with the YCp(Sc)PMA1,

YEp(Np)PMA4^{882Ochre}, or pFL36 (empty) plasmid (-) were grown for 3 days on solid medium with Pro as sole N source and Gal or Gluc as carbon source. **(B)** *GAL1p-PMA1 pma2Δ* cells expressing (Sc)Pma1 or (Np)Pma4^{882Ochre} from a plasmid (as in A) were grown on Gluc Pro medium in a microplate reader for forty hours. Data points represent averages of the OD at 660 nm of two biological replicates; error bars represent SD. **(C)** Strains and growth conditions as in B, except that the strains were also transformed with a plasmid (pHl-U) expressing *pHluorin*. The cytosolic pH was monitored during growth with or without addition, starting at 1 min, of FCCP (20 µM) for various times. **(D)** Left. Cells as in B but also expressing HA-Npr1 from a plasmid were grown on Gluc NH_4^+ medium. After a shift to Gluc Pro medium for three hours, [^{14}C]-β-ala (0.1 or 1 mM) was added to the medium before measuring the incorporated radioactivity at various times. Right. Strains and growth conditions as in left. Uptake via Gap1 of [^{14}C]-β-ala (provided at 0.1 mM to *(Sc)PMA1*-expressing cells and at 1 mM to *(Np)PMA4^{882Ochre}*-expressing cells) was measured before and after glucose starvation for 5 min or after addition of FCCP (20 µM) or its solvent alone (0.2% EtOH) for 5 min. Plotted values represent percentages of initial Gap1 activity, and correspond to means ± SD of two independent experiments. **(E)** Top. Strains and growth conditions as in D, except that the cells were collected before and 4 and 10 min after addition of β-ala (0.1 or 1 mM). Crude extracts were prepared and immunoblotted with anti-HA and anti-Pgk antibodies. Bottom. Same as in top panel, except that only *(Sc)PMA1*-expressing cells were collected and half of the culture was treated for 30 min with Rap. **(F)** Experiments similar to those in D, except that the cells harbored an empty *URA3* plasmid instead of the HA-Npr1 plasmid and were grown on Gluc Pro medium. **(G)** Top. Strains and growth conditions were as in F, and cells were treated as in E. Crude extracts were prepared and immunoblotted with anti-(P) T^{737}-Sch9 and anti-Sch9$_{Total}$ antibodies. Bottom. Same as in top panel except that *(Sc)PMA1*-expressing cells were collected and half of the culture was treated for 30 min with Rap. **(H-I)** Strains, growth conditions, and immuno-detection as in E except that cells were collected before and at various times after addition of FCCP (20 µM) or BAF (1 µM). **(J)** Rapamycin recovery assay for *GAL1p-PMA1 pma2Δ* cells expressing (Sc)Pma1 or (Np)Pma4^{882Ochre} from plasmids. Cells were treated or not with Rap (200 ng/ml) for 6 h, washed twice, plotted in 2-

fold serial dilutions on solid Gluc Pro medium, and incubated for 4 days. **(K)** w-t and *gtr1Δ gtr2Δ* cells expressing HA-Npr1 from a plasmid and *GAL1p-PMA1 pma2Δ* cells co-expressing (Sc)Pma1 or (Np)Pma4^{882Ochre} and HA-Npr1 from plasmids were grown on Gluc NH_4^+ medium. After a shift to Gluc Pro medium for three hours, cells were collected before and 30 min after addition of NH_4^+ (5 mM). Cells were also collected after addition of Rap for 30 min, followed by addition of NH_4^+ (5 mM) for 30 min. Crude extracts were prepared and immunoblotted with anti-HA and anti-Pgk antibodies.

Figure 1-supplement 1. Uptake of β-alanine promotes ubiquitylation and downregulation of the inactive Gap1-126 permease via TORC1-dependent stimulation of the Bul arrestins (A) *gap1Δ BUL2-HA* cells expressing Gap1 from a plasmid were grown on Gluc Pro medium and NH_4^+ (20 mM) or β-ala (0.5 mM) was added to the culture for 4 min. Rap was added to half of the culture for 30 min before addition of NH_4^+ or β-ala. Crude cell extracts were immunoblotted with anti-HA and anti-Pgk antibodies. The results show that the Rap-sensitive change in Bul2-HA migration upon addition of NH_4^+, previously shown to reflect its dephosphorylation and monoubiquitylation (Merhi et al. 2012), also occurs upon addition of β-ala. Addition of β-ala thus activates TORC1. **(B)** w-t, *gap1Δ*, *npi1-1/rsp5,* and *bul1Δ bul2Δ* cells expressing the inactive Gap1-126-GFP from a plasmid, and w-t cells expressing Gap1-126(K9R-K16R)-GFP also from a plasmid, were grown on Gal Pro medium. Glucose was added for 30 min to stop Gap1-126 or Gap1-126(K9R,K16R) neosynthesis prior to β-ala addition (0.5 mM) for 4 min. Crude cell extracts were prepared and immunoblotted with anti-GFP and anti-Pma1 antibodies. The results show that addition of β-ala induces the appearance of the typical two upper bands corresponding to ubiquitylated forms of Gap1. As expected, this ubiquitylation is impaired if the two Ub acceptor lysines (K9 and K16) of the permease are mutated. Ubiquitylation of Gap1-126 is impaired in the *gap1Δ*, *bul1Δ bul2Δ* and hypomorphic *npi1/rsp5* mutants. Uptake of β-ala via the endogenous Gap1 permease thus promotes Ub-dependent downregulation of the inactive Gap1-126 protein **(C)** Left. w-t and *gap1Δ* cells expressing Gap1-126-GFP from a plasmid were grown on Gal Pro medium. Glucose was supplied for 30 min to stop Gap1 neosynthesis. [^{14}C]-β-ala (0.5 mM) was added to the medium before measuring the incorporated radioactivity at various times. The result shows that [^{14}C]-β-ala is incorporated into cells expressing the endogenous Gap1 permease. Right. Fluorescence microscopy analysis of cells in panel C. Cells were grown on Gal Pro medium. Glucose was added for 1.5 h to stop Gap1 neosynthesis, and β-ala (0.5 mM) was added for 30 min or 1 h before analysis by fluorescence microscopy. CMAC staining (blue) was used to highlight the vacuole. The result shows that uptake of β-ala by Gap1 elicits endocytosis of the inactive Gap1-126-GFP protein.

Figure 1-supplement 2. An anti-(P) T^{737}-Sch9 antibody recognizes phosphorylated Sch9 after NH_4^+ addition. w-t cells transformed with pFL38 (URA3) and *sch9Δ* cells (JW00035) co-transformed with pCJ366 (TRP1-LEU2-HIS3) and pFL38 (URA3) were grown on Gluc Pro medium (for JW00035 cells, the growth medium was supplemented with adenine to compensate for the *ade2* auxotrophy). Cells pre-incubated or not with Rap for 30 min were collected before and 10 and 30 min after addition of NH_4^+ (20 mM). Crude extracts were prepared and immunoblotted with anti-(P) T^{737}-Sch9 and anti-$Sch9_{Total}$ antibodies. The immunoblot shows that the anti-(P) T^{737}-Sch9 antibody recognized a band corresponding to a molecular mass of ~125 KDa, whose intensity increased after NH_4^+ addition. This band was not detected in Rap-treated w-t cells or in cells of the *sch9Δ* mutant strain. The same antibody also revealed a nonspecific band corresponding to a higher molecular mass, which can be used as a loading control. As expected, the anti-$Sch9_{Total}$ antibody recognized Sch9 even in Rap-treated cells.

Figure 5-supplement 1. Addition of the FCCP uncoupler stimulates trehalase activity in N-deprived cells. w-t cells were incubated for 16 h in Gluc medium (pH 6.1) devoid of any N source. FCCP (20 μM) or its solvent (0.2% EtOH, control) was added to the cells and trehalase activity was measured in cell samples collected at various times. Plotted values represent means ± SD of three independent experiments.

Figure 7-supplement 1. $Pma4^{882Ochre}$ from tobacco fails to compensate for the lack of Pma1 as regards TORC1 activation in a *pma1Δ pma2Δ* mutant (A) Left. The *pma1Δ pma2Δ* strain co-transformed with the YCp(Sc)PMA1 or YEp(Np)$PMA4^{882Ochre}$ plasmid and a *LEU2-HIS3-LYS2* (pCJ315) plasmid were grown on Gluc Pro medium (pH = 6.5) containing 0.00225 % adenine to compensate for the *ade2* auxotrophy. [^{14}C]-β-ala was added (at 0.1 mM to *(Sc)PMA1*-expressing cells, at 1 mM to *(Np)*$PMA4^{882Ochre}$-expressing cells) before measuring the incorporated radioactivity at various times. Right. Strains and growth conditions as in the left panel. Percentages of initial Gap1 activity were calculated after glucose starvation for 5 min, or after addition of FCCP (20 μM) or EtOH (0.2%) for 5 min. Plotted values

represent means ± SD of two independent experiments. **(B)** Top. Strains and growth conditions as in A. Cells were collected before and 4 and 10 min after addition of β-ala (as in A). Crude extracts were prepared and immunoblotted with anti-(P) T^{737}-Sch9 and anti-$Sch9_{Total}$ antibodies. Bottom. Same as in the previous experiment, except that *(Sc)PMA1*-expressing cells were treated or not with Rap for 30 min before addition of β-ala (0.1 mM).

Figure 7-supplement 2. TORC1 is not stimulated by Gln, Leu, or Arg, transported into $Pma4^{882Ochre}$ expressing cells (A) *GAL1p-PMA1 pma2Δ* cells co-expressing (Sc)Pma1 or (Np)$Pma4^{882Ochre}$ and HA-Npr1 from plasmids were grown on Gluc NH_4^+ medium. After a shift to Gluc Pro medium for three hours, [^{14}C]-L-Gln (0.012 mM to *(Sc)PMA1*-expressing cells, 0.4 mM to *(Np)*$PMA4^{882Ochre}$ cells) was added to the medium before measuring the incorporated radioactivity at various times. **(B)** Top left. Strains and growth conditions as in A, except that the cells were collected before and 4 and 10 min after addition of Gln. Crude extracts were prepared and immunoblotted with anti-HA and anti-Pgk antibodies. Top right. Same as in top left, except that only *(Sc)PMA1*-expressing cells were collected and half of the culture was treated for 30 min with Rap. Bottom. w-t and *gtr1Δ gtr2Δ* cells expressing HA-Npr1 from a plasmid were grown on Gluc Pro medium. Cells were collected before and 4 and 10 min after addition of Gln (0.5 mM). Crude extracts were prepared and immunoblotted with anti-HA and anti-Pgk antibodies. **(C and D)** and **(E and F)** Same as in A and B except that Leu and Arg were added instead of Gln, respectively. The concentrations used for Leu and Arg are indicated in the figure. In the experiment comparing the *w-t* and *gtr1Δ gtr2Δ* strains, Leu and Arg were added at a final concentration of 0.5 mM.

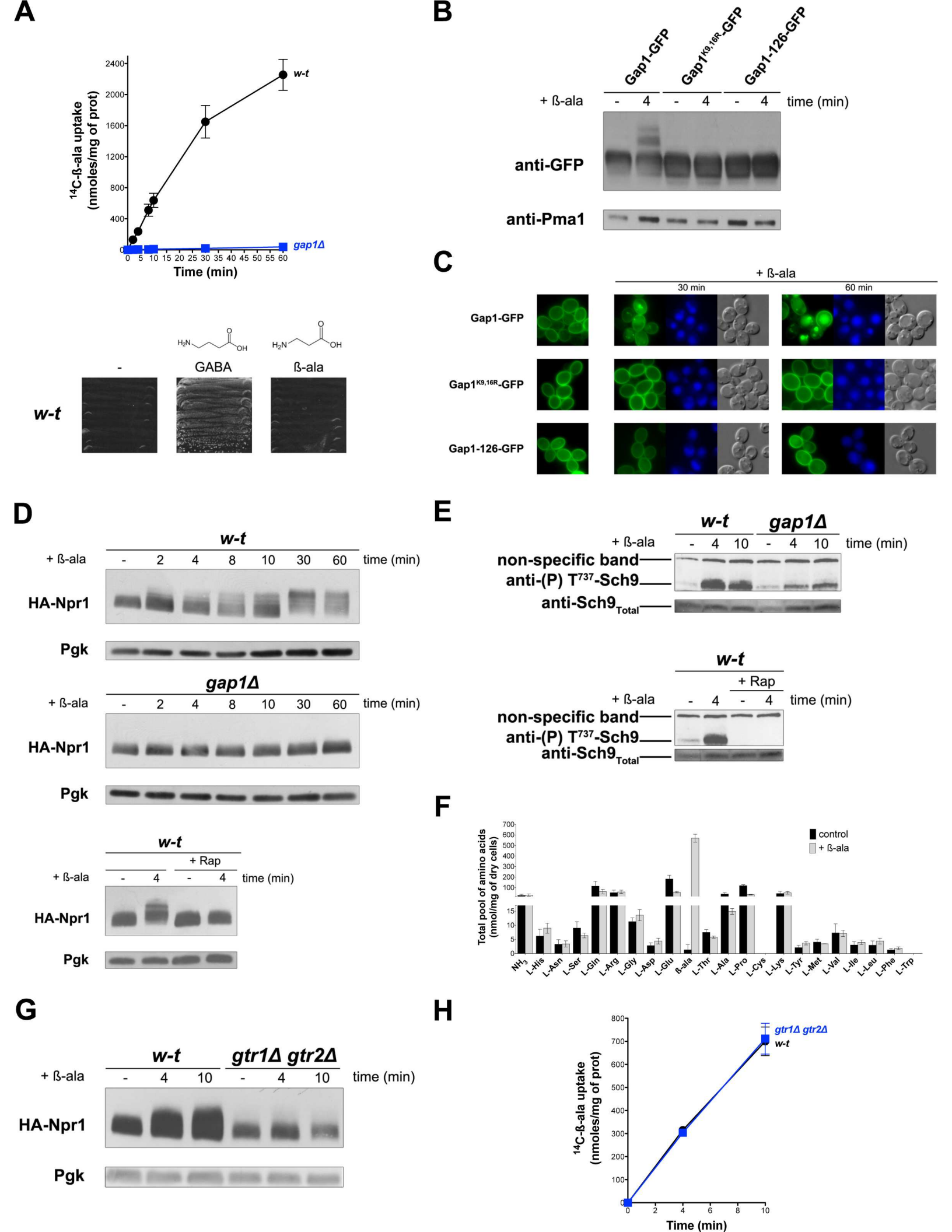
A
^{14}C-ß-ala uptake (nmoles/mg of prot)
Time (min)
w-t
gap1Δ
GABA
ß-ala
w-t
B
Gap1-GFP
Gap1^{K9,16R}-GFP
Gap1-126-GFP
+ ß-ala
time (min)
anti-GFP
anti-Pma1
C
+ ß-ala
30 min
60 min
Gap1-GFP
Gap1^{K9,16R}-GFP
Gap1-126-GFP
D
w-t
gap1Δ
+ ß-ala
time (min)
HA-Npr1
Pgk
+ Rap
E
non-specific band
anti-(P) T^{737}-Sch9
anti-Sch9$_{Total}$
F
Total pool of amino acids (nmol/mg of dry cells)
control
+ ß-ala
NH$_3$ L-His L-Asn L-Ser L-Gln L-Arg L-Gly L-Asp L-Glu ß-ala L-Thr L-Ala L-Pro L-Cys L-Lys L-Tyr L-Met L-Val L-Ile L-Leu L-Phe L-Trp
G
gtr1Δ gtr2Δ
H
gtr1Δ gtr2Δ
w-t

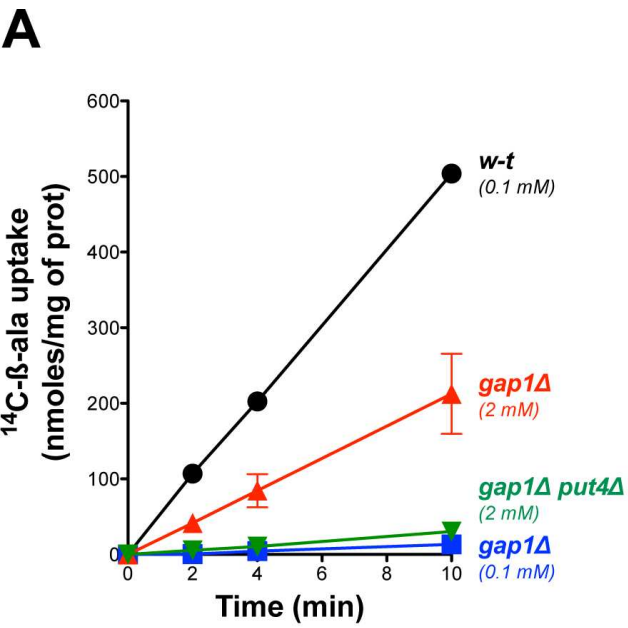
A
600
500
400
300
200
100
0
0
2
4
6
8
10
^{14}C-ß-ala uptake
(nmoles/mg of prot)
Time (min)
w-t
(0.1 mM)
gap1Δ
(2 mM)
gap1Δ put4Δ
(2 mM)
gap1Δ
(0.1 mM)

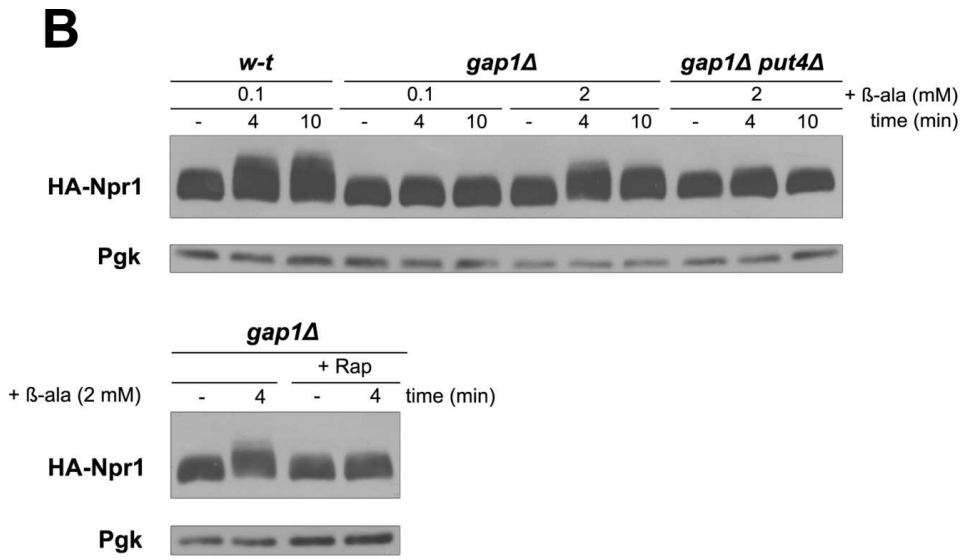
B
w-t
gap1Δ
gap1Δ put4Δ
0.1
0.1
2
2
+ ß-ala (mM)
- 4 10 - 4 10 - 4 10 - 4 10
time (min)
HA-Npr1
Pgk
gap1Δ
+ Rap
+ ß-ala (2 mM)
- 4 - 4
time (min)
HA-Npr1
Pgk

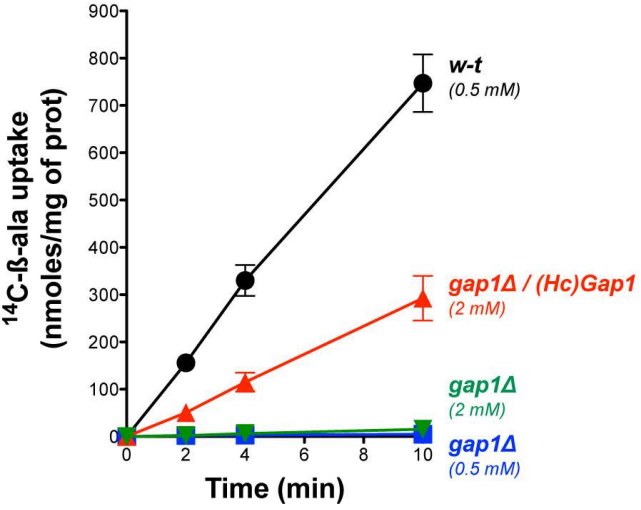
C
900
800
700
600
500
400
300
200
100
0
0
2
4
6
8
10
^{14}C-ß-ala uptake
(nmoles/mg of prot)
Time (min)
w-t
(0.5 mM)
gap1Δ / (Hc)Gap1
(2 mM)
gap1Δ
(2 mM)
gap1Δ
(0.5 mM)

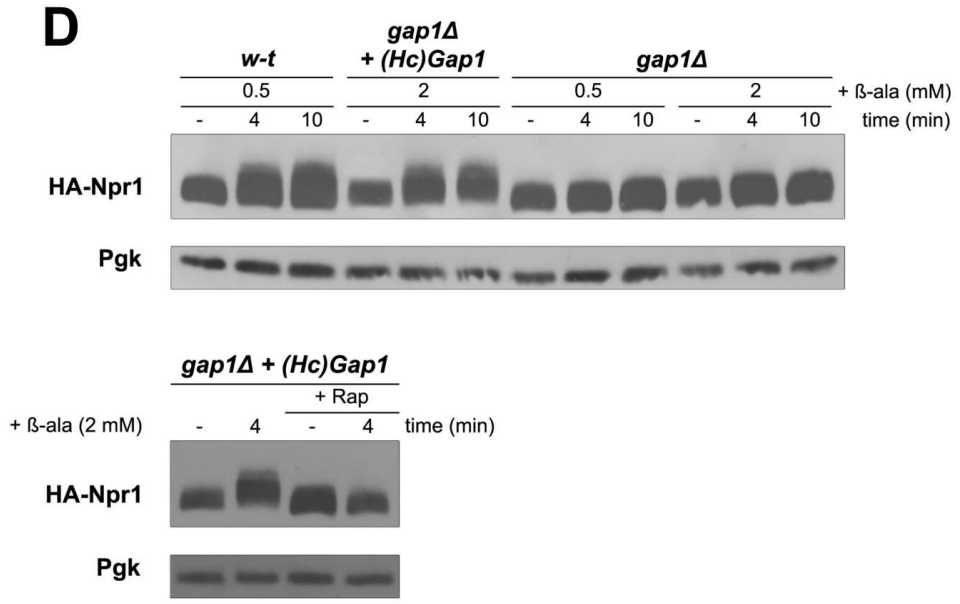
D
w-t
gap1Δ
+ (Hc)Gap1
gap1Δ
0.5
2
0.5
2
+ ß-ala (mM)
- 4 10 - 4 10 - 4 10 - 4 10
time (min)
HA-Npr1
Pgk
gap1Δ + (Hc)Gap1
+ Rap
+ ß-ala (2 mM)
- 4 - 4
time (min)
HA-Npr1
Pgk

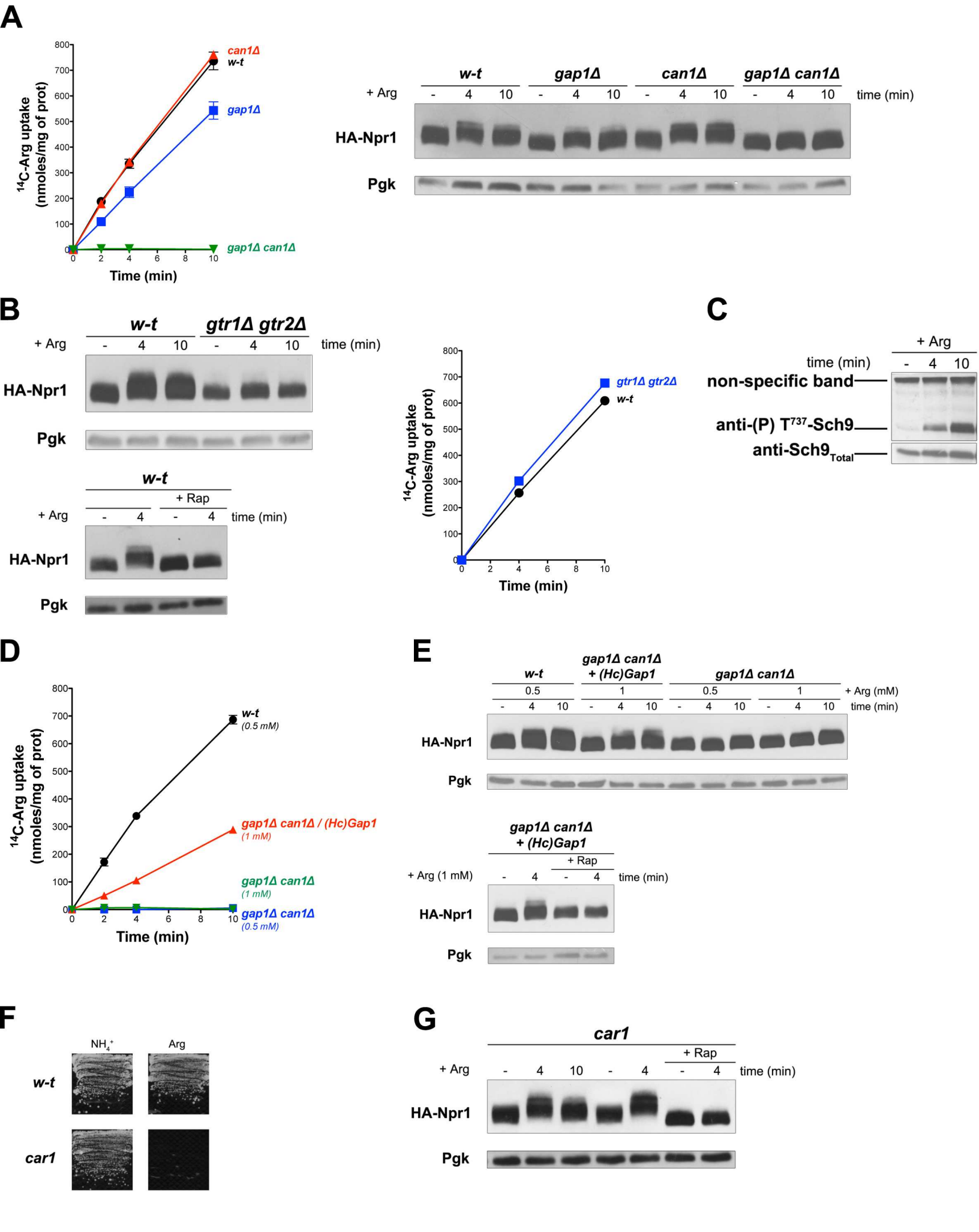
A
^{14}C-Arg uptake (nmoles/mg of prot)
Time (min)
can1Δ
w-t
gap1Δ
gap1Δ can1Δ
w-t
gap1Δ
can1Δ
gap1Δ can1Δ
+ Arg
time (min)
HA-Npr1
Pgk
B
w-t
gtr1Δ gtr2Δ
+ Arg
time (min)
HA-Npr1
Pgk
w-t
+ Rap
+ Arg
time (min)
HA-Npr1
Pgk
gtr1Δ gtr2Δ
w-t
^{14}C-Arg uptake (nmoles/mg of prot)
Time (min)
C
+ Arg
time (min)
non-specific band
anti-(P) T^{737}-Sch9
anti-Sch9$_{Total}$
D
^{14}C-Arg uptake (nmoles/mg of prot)
Time (min)
w-t
(0.5 mM)
gap1Δ can1Δ / (Hc)Gap1
(1 mM)
gap1Δ can1Δ
(1 mM)
gap1Δ can1Δ
(0.5 mM)
E
w-t
gap1Δ can1Δ
+ (Hc)Gap1
gap1Δ can1Δ
+ Arg (mM)
time (min)
HA-Npr1
Pgk
gap1Δ can1Δ
+ (Hc)Gap1
+ Rap
+ Arg (1 mM)
time (min)
HA-Npr1
Pgk
F
NH$_4^+$
Arg
w-t
car1
G
car1
+ Rap
+ Arg
time (min)
HA-Npr1
Pgk

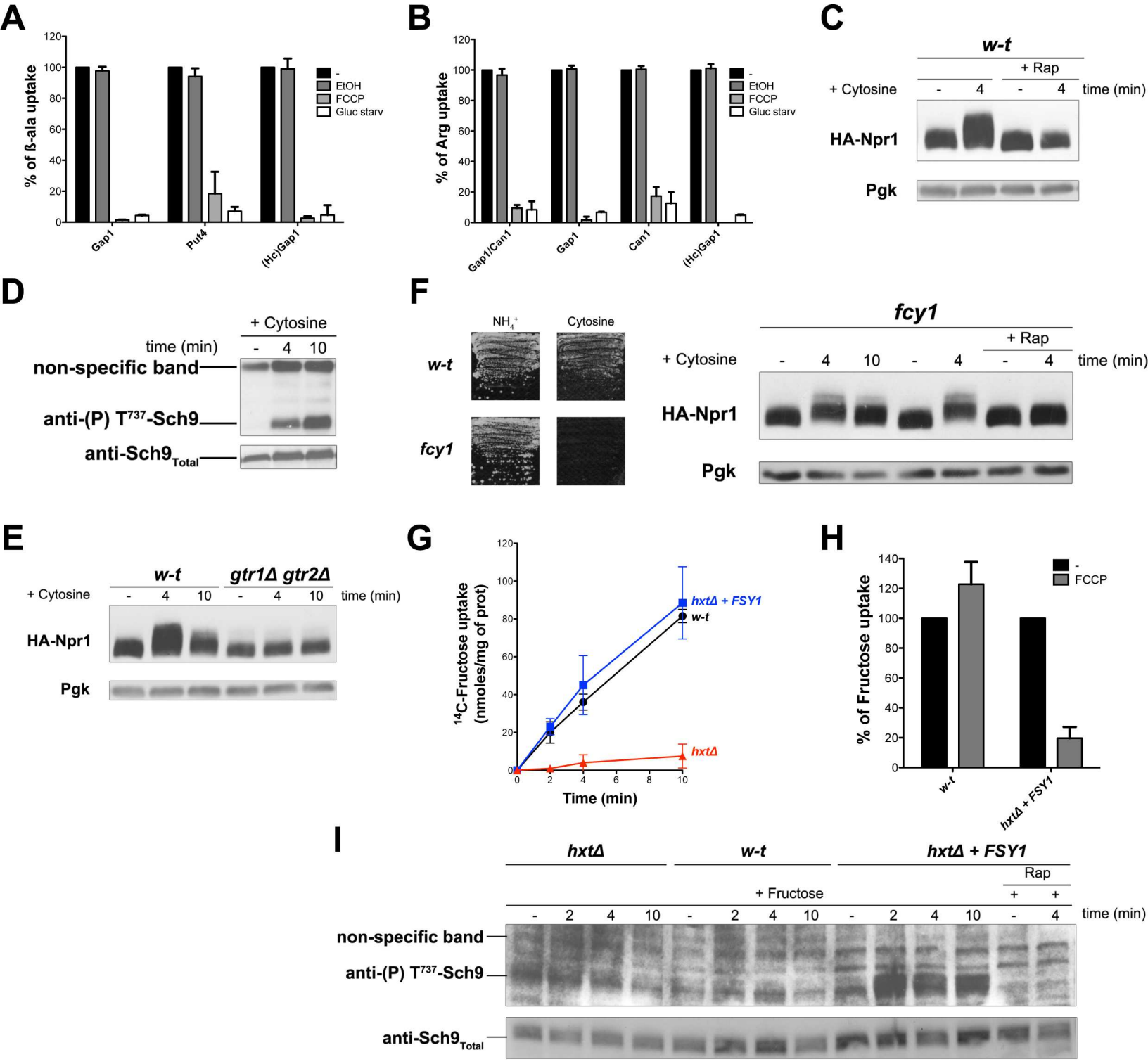
A
% of ß-ala uptake
120
100
80
60
40
20
0
-
EtOH
FCCP
Gluc starv
Gap1
Put4
(Hc)Gap1
B
% of Arg uptake
120
100
80
60
40
20
0
-
EtOH
FCCP
Gluc starv
Gap1/Can1
Gap1
Can1
(Hc)Gap1
C
w-t
+ Rap
+ Cytosine
- 4 - 4
time (min)
HA-Npr1
Pgk
D
+ Cytosine
time (min)
- 4 10
non-specific band
anti-(P) T737-Sch9
anti-Sch9Total
F
NH4+
Cytosine
w-t
fcy1
fcy1
+ Rap
+ Cytosine
- 4 10 - 4 - 4
time (min)
HA-Npr1
Pgk
E
w-t
gtr1Δ gtr2Δ
+ Cytosine
- 4 10 - 4 10
time (min)
HA-Npr1
Pgk
G
14C-Fructose uptake (nmoles/mg of prot)
120
100
80
60
40
20
0
0 2 4 6 8 10
Time (min)
hxtΔ + FSY1
w-t
hxtΔ
H
% of Fructose uptake
140
120
100
80
60
40
20
0
-
FCCP
w-t
hxtΔ + FSY1
I
hxtΔ
w-t
hxtΔ + FSY1
Rap
+ Fructose
+ +
- 2 4 10 - 2 4 10 - 2 4 10 - 4
time (min)
non-specific band
anti-(P) T737-Sch9
anti-Sch9Total

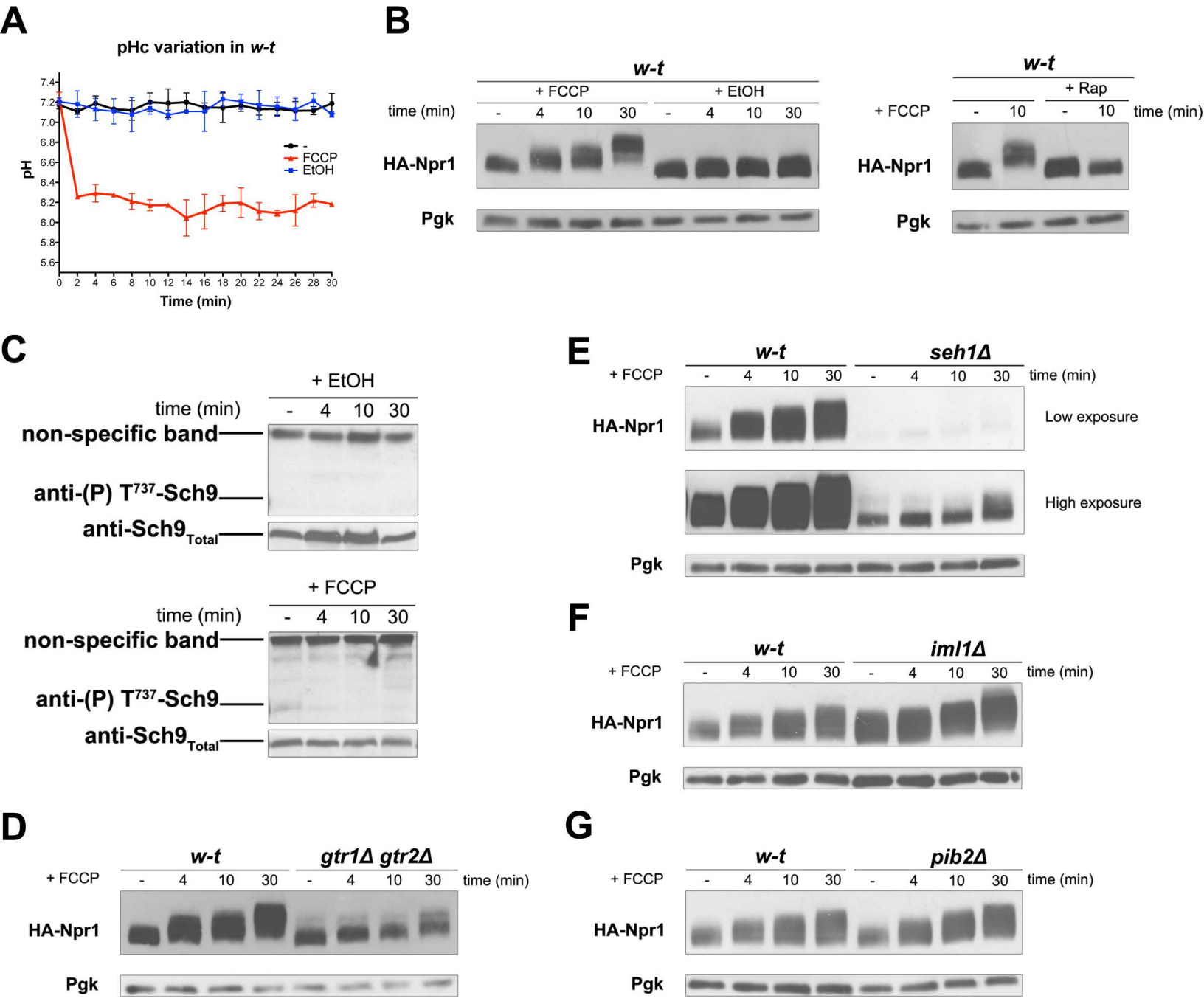
A
pHc variation in w-t
pH
Time (min)
-
FCCP
EtOH
B
w-t
+ FCCP
+ EtOH
time (min)
HA-Npr1
Pgk
w-t
+ Rap
+ FCCP
time (min)
HA-Npr1
Pgk
C
+ EtOH
time (min)
non-specific band
anti-(P) T737-Sch9
anti-Sch9Total
+ FCCP
time (min)
non-specific band
anti-(P) T737-Sch9
anti-Sch9Total
D
w-t
gtr1Δ gtr2Δ
+ FCCP
time (min)
HA-Npr1
Pgk
E
w-t
seh1Δ
+ FCCP
time (min)
HA-Npr1
Low exposure
High exposure
Pgk
F
w-t
iml1Δ
+ FCCP
time (min)
HA-Npr1
Pgk
G
w-t
pib2Δ
+ FCCP
time (min)
HA-Npr1
Pgk

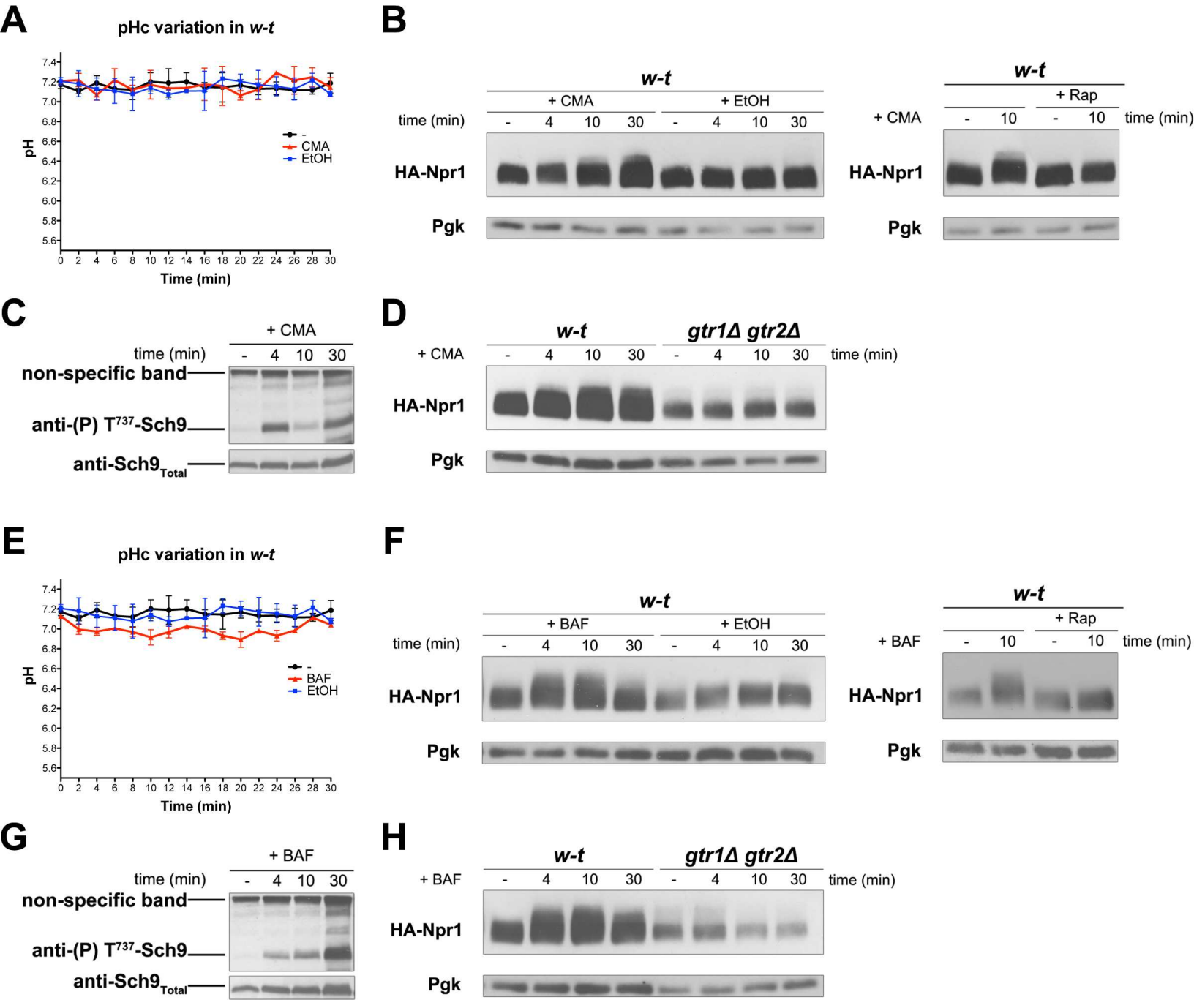
A
pHc variation in w-t
pH
Time (min)
-
CMA
EtOH
B
w-t
+ CMA
+ EtOH
time (min)
HA-Npr1
Pgk
+ Rap
C
+ CMA
non-specific band
anti-(P) T737-Sch9
anti-Sch9Total
D
w-t
gtr1Δ gtr2Δ
E
pHc variation in w-t
BAF
F
+ BAF
G
H

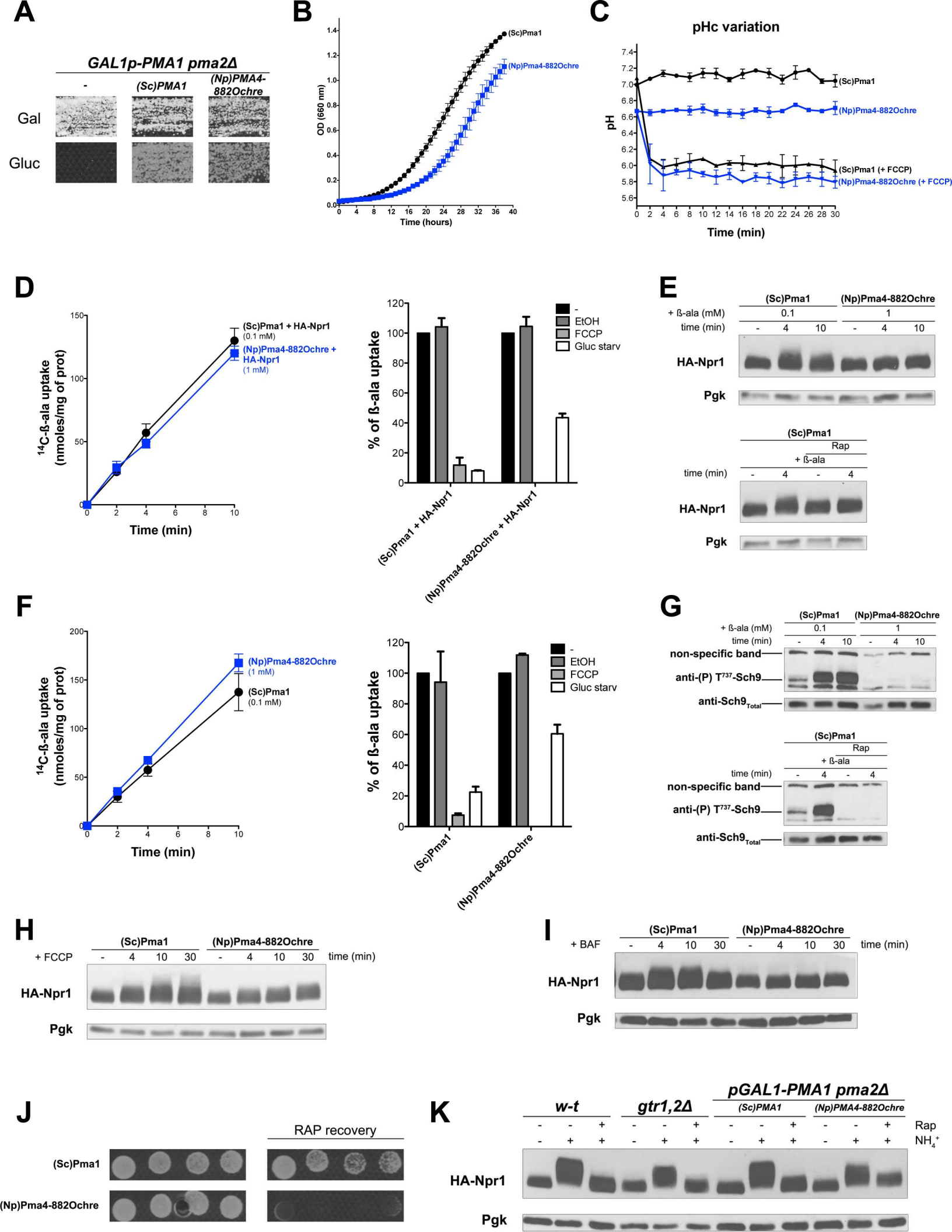
A
GAL1p-PMA1 pma2Δ
-
(Sc)PMA1
(Np)PMA4-882Ochre
Gal
Gluc
B
OD (660 nm)
Time (hours)
(Sc)Pma1
(Np)Pma4-882Ochre
C
pHc variation
pH
Time (min)
(Sc)Pma1
(Np)Pma4-882Ochre
(Sc)Pma1 (+ FCCP)
(Np)Pma4-882Ochre (+ FCCP)
D
14C-ß-ala uptake (nmoles/mg of prot)
Time (min)
(Sc)Pma1 + HA-Npr1 (0.1 mM)
(Np)Pma4-882Ochre + HA-Npr1 (1 mM)
% of ß-ala uptake
-
EtOH
FCCP
Gluc starv
(Sc)Pma1 + HA-Npr1
(Np)Pma4-882Ochre + HA-Npr1
E
(Sc)Pma1
(Np)Pma4-882Ochre
+ ß-ala (mM)
0.1
1
time (min)
HA-Npr1
Pgk
Rap
+ ß-ala
F
14C-ß-ala uptake (nmoles/mg of prot)
Time (min)
(Np)Pma4-882Ochre (1 mM)
(Sc)Pma1 (0.1 mM)
% of ß-ala uptake
-
EtOH
FCCP
Gluc starv
(Sc)Pma1
(Np)Pma4-882Ochre
G
non-specific band
anti-(P) T737-Sch9
anti-Sch9Total
H
+ FCCP
time (min)
HA-Npr1
Pgk
I
+ BAF
time (min)
HA-Npr1
Pgk
J
RAP recovery
(Sc)Pma1
(Np)Pma4-882Ochre
K
w-t
gtr1,2Δ
pGAL1-PMA1 pma2Δ
(Sc)PMA1
(Np)PMA4-882Ochre
Rap
NH4+
HA-Npr1
Pgk

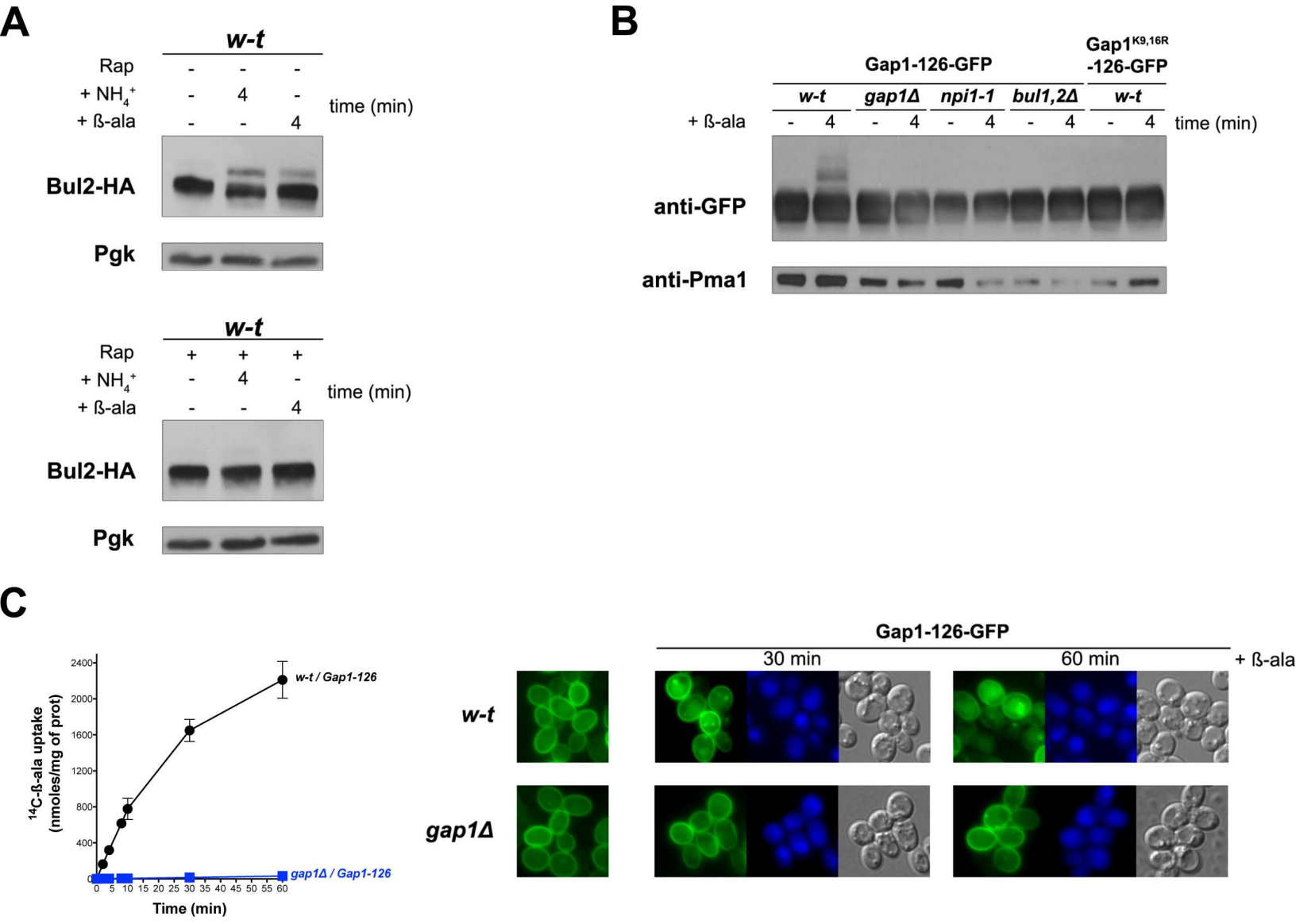
A
w-t
Rap - - -
+ NH4+ - 4 -
+ ß-ala - - 4
time (min)
Bul2-HA
Pgk
w-t
Rap + + +
+ NH4+ - 4 -
+ ß-ala - - 4
time (min)
Bul2-HA
Pgk
B
Gap1-126-GFP
Gap1K9,16R -126-GFP
w-t
gap1Δ
npi1-1
bul1,2Δ
w-t
+ ß-ala - 4 - 4 - 4 - 4 - 4
time (min)
anti-GFP
anti-Pma1
C
14C-ß-ala uptake (nmoles/mg of prot)
2400
2000
1600
1200
800
400
0
w-t / Gap1-126
gap1Δ / Gap1-126
0 5 10 15 20 25 30 35 40 45 50 55 60
Time (min)
Gap1-126-GFP
30 min
60 min
+ ß-ala
w-t
gap1Δ

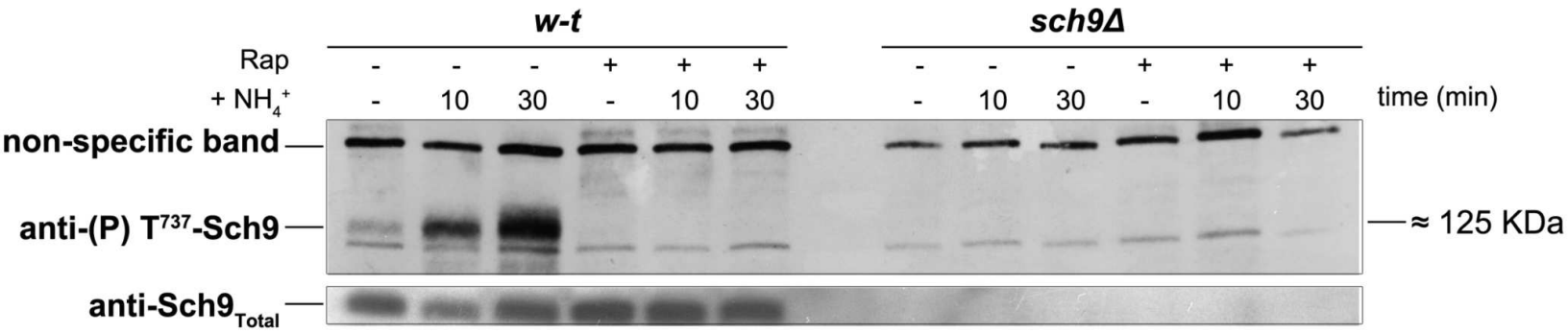
w-t
sch9Δ
Rap
+ NH4+
- - - + + + - - - + + +
- 10 30 - 10 30 - 10 30 - 10 30
time (min)
non-specific band
anti-(P) T737-Sch9
anti-Sch9Total
≈ 125 KDa

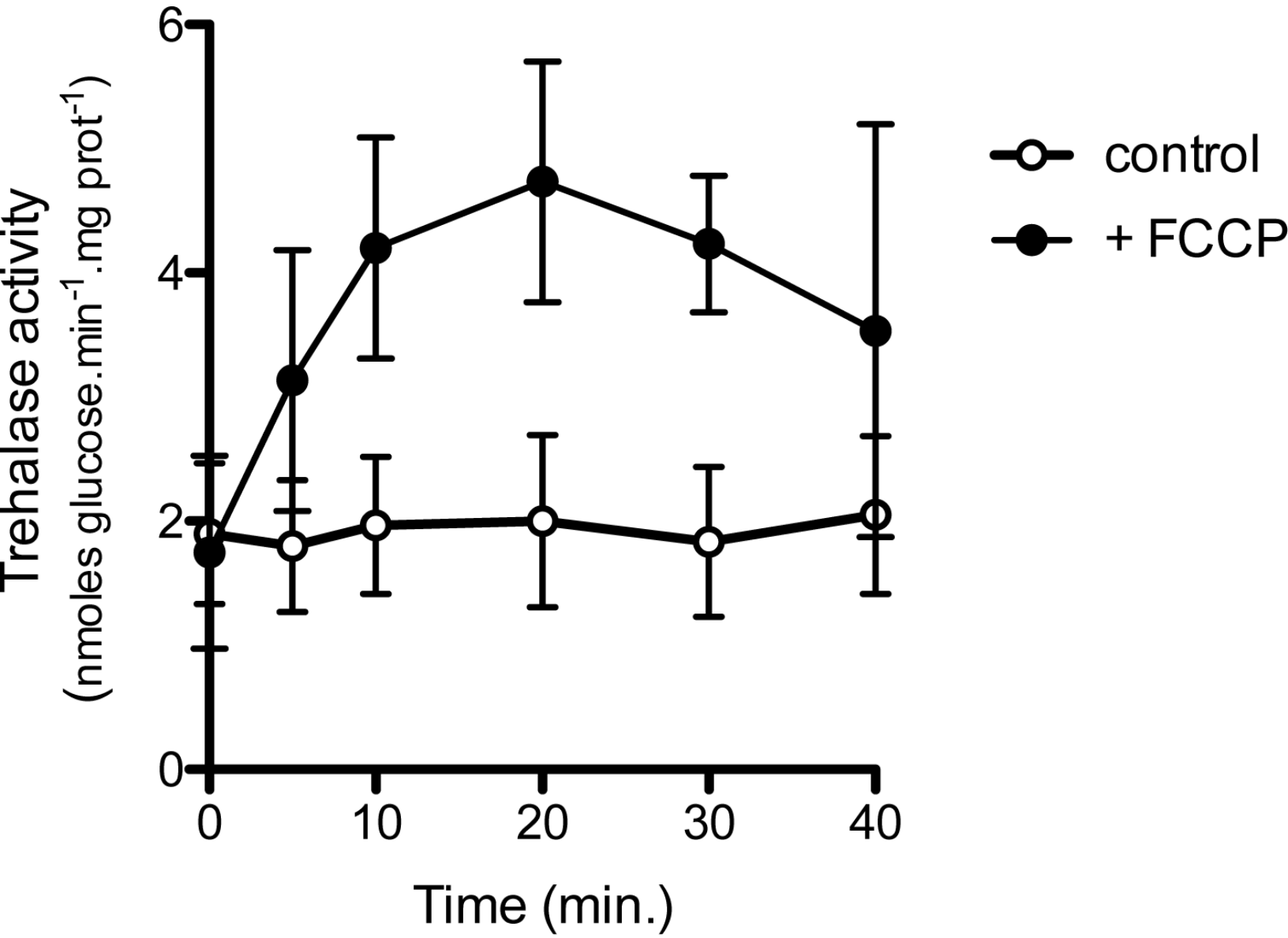
Trehalase activity
(nmoles glucose.min-1.mg prot-1)
6
4
2
0
0
10
20
30
40
Time (min.)
control
+ FCCP

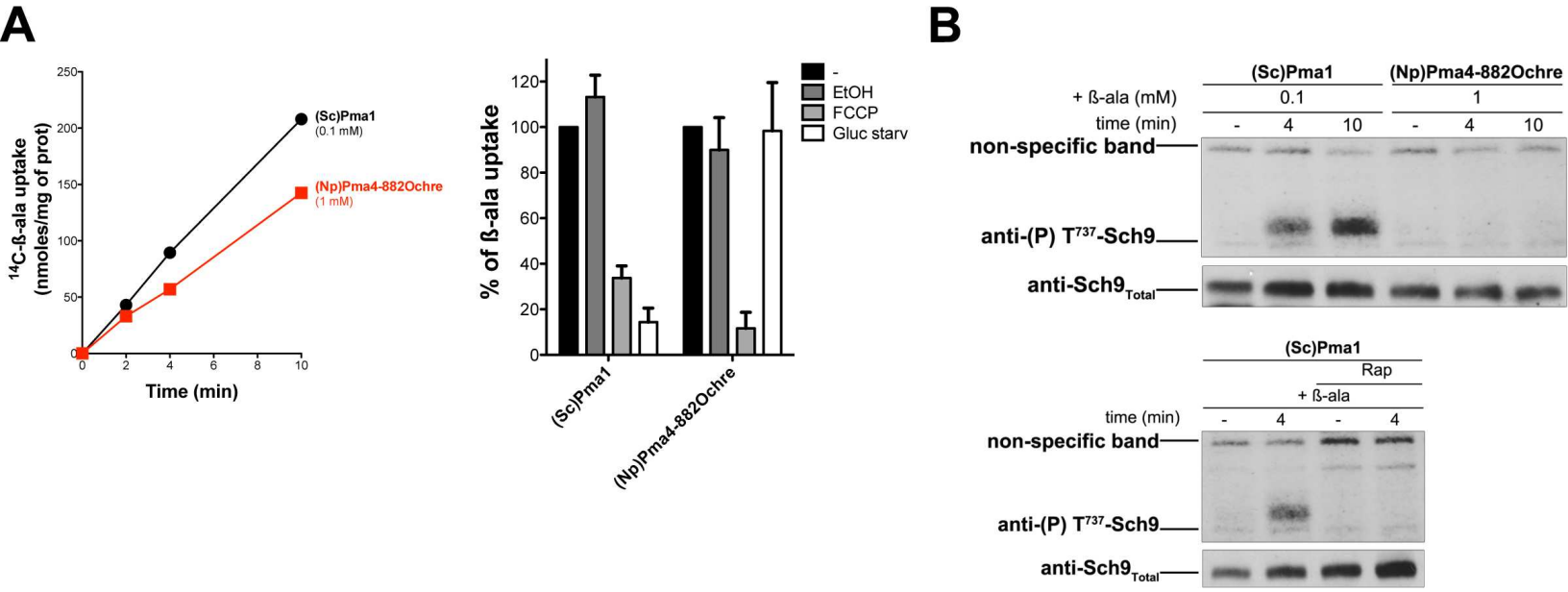
A
^{14}C-ß-ala uptake (nmoles/mg of prot)
Time (min)
(Sc)Pma1
(0.1 mM)
(Np)Pma4-882Ochre
(1 mM)
% of ß-ala uptake
-
EtOH
FCCP
Gluc starv
(Sc)Pma1
(Np)Pma4-882Ochre
B
(Sc)Pma1
(Np)Pma4-882Ochre
+ ß-ala (mM)
0.1
1
time (min)
non-specific band
anti-(P) T737-Sch9
anti-Sch9Total
Rap
+ ß-ala

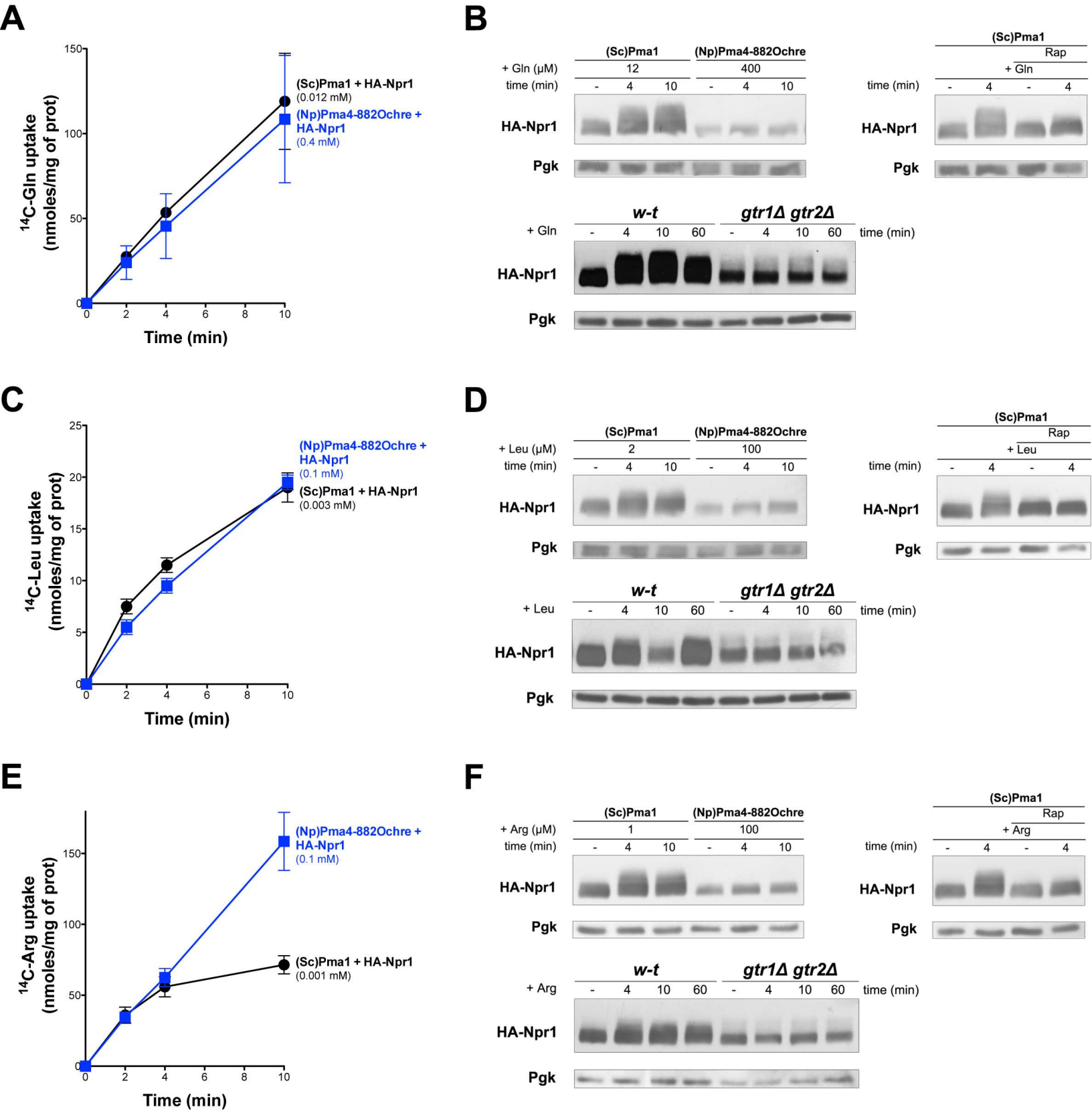
A
B
C
D
E
F
^{14}C-Gln uptake (nmoles/mg of prot)
Time (min)
(Sc)Pma1 + HA-Npr1 (0.012 mM)
(Np)Pma4-882Ochre + HA-Npr1 (0.4 mM)
(Sc)Pma1
(Np)Pma4-882Ochre
+ Gln (µM)
12
400
time (min)
HA-Npr1
Pgk
Rap
+ Gln
w-t
gtr1Δ gtr2Δ
^{14}C-Leu uptake (nmoles/mg of prot)
(Np)Pma4-882Ochre + HA-Npr1 (0.1 mM)
(Sc)Pma1 + HA-Npr1 (0.003 mM)
+ Leu (µM)
2
100
+ Leu
^{14}C-Arg uptake (nmoles/mg of prot)
(Np)Pma4-882Ochre + HA-Npr1 (0.1 mM)
(Sc)Pma1 + HA-Npr1 (0.001 mM)
+ Arg (µM)
1
100
+ Arg